5101-220
Flat-Plate
Solar Array Project

DOE/JPL-1012-87

Applications of Ethylene Vinyl Acetate as an Encapsulation Material for Terrestrial Photovoltaic Modules

E.F. Cuddihy
C.D. Coulbert
R.H. Liang
A. Gupta
P. Willis
B. Baum

April 15, 1983

Prepared for
U.S. Department of Energy
Through an Agreement with
National Aeronautics and Space Administration
by
Jet Propulsion Laboratory
California Institute of Technology
Pasadena, California

JPL PUBLICATION 83-35

5101-220
DOE/JPL-1012-87
Flat-Plate
Solar Array Project

Applications of Ethylene Vinyl Acetate as an Encapsulation Material for Terrestrial Photovoltaic Modules

E.F. Cuddihy
C.D. Coulbert
R.H. Liang
A. Gupta
P Willis
B. Baum

April 15, 1983

Prepared for
U S Department of Energy
Through an Agreement with
National Aeronautics and Space Administration
by
Jet Propulsion Laboratory
California Institute of Technology
Pasadena, California

JPL PUBLICATION 83-35

Prepared by the Jet Propulsion Laboratory, California Institute of Technology, for the U.S. Department of Energy through an agreement with the National Aeronautics and Space Administration.

The JPL Flat-Plate Solar Array Project is sponsored by the U.S. Department of Energy and is part of the Photovoltaic Energy Systems Program to initiate a major effort toward the development of cost-competitive solar arrays.

This publication reports on work done under NASA Task RD-152, Amendment 66, DOE/NASA IAA No. DE-AI01-76ET20356.

ABSTRACT

Terrestrial photovoltaic modules must undergo substantial reductions in cost in order to become economically attractive as practical devices for large-scale production of electricity. Part of the cost reductions must be realized by the encapsulation materials that are used to package, protect, and support the solar cells, electrical interconnects, and other ancillary components. As many of the encapsulation materials are polymeric, cost reductions necessitate the use of low-cost polymers. The performance and current status of ethylene vinyl acetate, a low-cost polymer that is being investigated as an encapsulation material for terrestrial photovoltaic modules, are described.

CONTENTS

Figures

Tables

SECTION I

INTRODUCTION

Photovoltaic (PV) modules contain strings of electrically interconnected solar cells capable of producing practical quantities of electricity when irradiated by sunlight. Silicon solar cells are fragile and are especially sensitive to brittle failure in tension and bending. In addition, the electrically conductive metallization materials (functioning as grids, interconnects, bus bars, and terminals) must be protected from atmospheric corrosion or other deteriorating interaction with the terrestrial environment. In short, the silicon solar cells must be mechanically supported, and the electrically conductive metallization materials must be isolated from environmental exposure.

Encapsulation materials are defined as all construction materials (excluding cells and electrical conductors) required in a PV module to provide mechanical support and environmental isolation. Early encapsulation efforts to identify a single material that could satisfy all of the encapsulation requirements and needs were unsuccessful (References 1, 2, and 3). The understanding evolved that more than one material would have to be assembled in a composite package to fabricate an encapsulation module satisfying all of the requirements.

After an examination of all commercial and experimental flat-plate module designs, it was found that these designs could be separated into two basic classes (see Figure 1). These are designated as substrate-bonded and superstrate-bonded designs, referring to the method by which the solar cells are supported mechanically. In the substrate design, the cells are supported by a structural substrate panel, and in the superstrate design the cells are supported by a transparent structural superstrate (i.e., glass).

From these two design options, nine basic encapsulation construction elements can be identified, which are illustrated in Figure 2 along with their designations and encapsulation functions. Fabricated modules need not use all nine of these construction elements, but combinations of these basic elements are incorporated in most module designs. However, all experimental and commercial modules of any design employ an elastomeric pottant. Before 1980, almost all commercial modules used either polyvinyl butyral (PVB) or silicone as pottant materials.

One objective of the Flat-Plate Solar Array Project (FSA), managed by the Jet Propulsion Laboratory (JPL) for the U.S. Department of Energy (DOE), was to demonstrate technical feasibility and 20-yr service life potential of photovoltaic modules fabricated with the lowest-costing materials that could fulfill the functions of encapsulation construction elements. Under this guideline, four low-cost elastomers have been identified or developed for potential application as pottant materials (References 2 through 8). One of the low-cost elastomers is ethylene vinyl acetate (EVA). This document describes the current status of EVA as an encapsulation pottant for terrestrial photovoltaic modules.

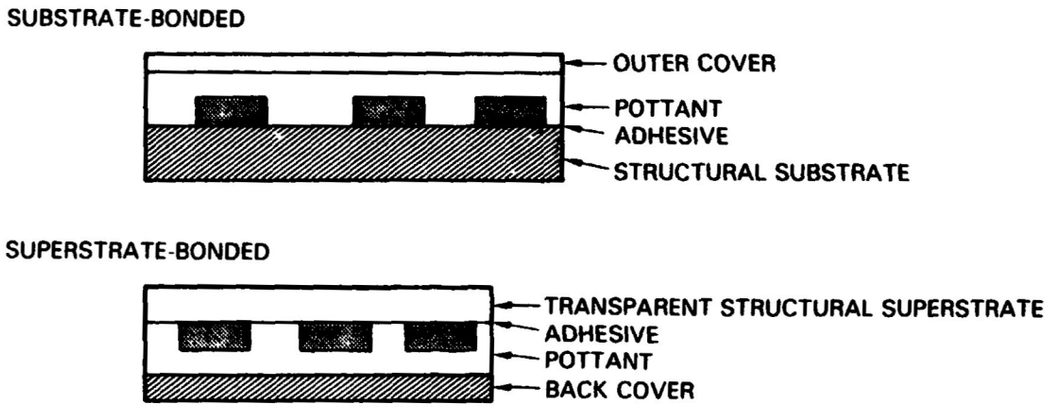

Figure 1. Flat-Plate Module Design Classifications

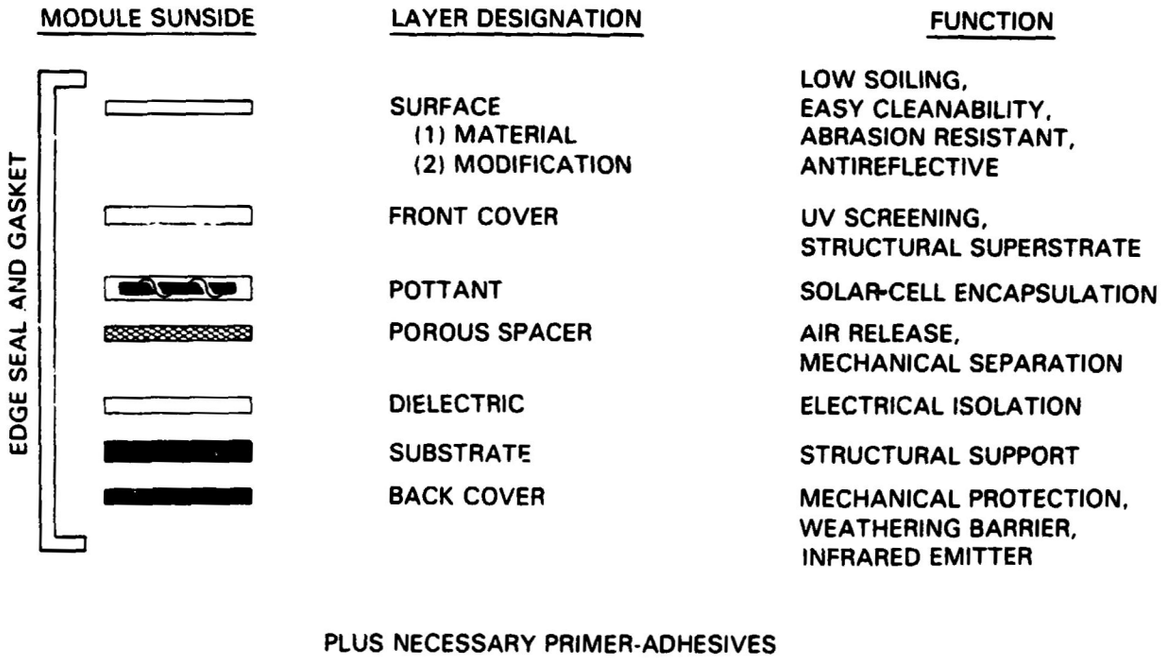

Figure 2. Encapsulation Materials: Module Construction Elements

SECTION II

ENCAPSULATION POTTANT: DEFINITION AND REQUIREMENTS

The central core of an encapsulation system is the pottant, a transparent, polymeric material that is the actual encapsulation material in a module. As there is a significant difference between the thermal-expansion coefficients of polymeric materials and of silicon cells and metallic interconnects, stresses developed from the thousands of daily thermal cycles can result in fractured cells, broken interconnects, or cracks and separations in the pottant material. To avoid these problems, the pottant material must not overstress the cell and interconnects, and must itself be resistant to fracture. From the results of a theoretical analysis (Reference 9), experimental efforts (References 1 and 3), and observations of the materials of choice used for pottants in commercial modules, it was concluded that the pottant must be a low-modulus, elastomeric material.

Also, these materials must be transparent, processible, and commercially available, and desirably low in cost. In many cases, the commercially available candidate material may not be physically or chemically suitable for direct encapsulation use, and therefore must also be amenable to low-cost modification. The pottant materials must have either inherent weatherability (retention of transparency and mechanical integrity under weather extremes) or the potential for long life that can be provided by cost-effective protection incorporated into the material or the module design.

In a fabricated module, the pottant provides three critical functions for module life and reliability:

(1) Maximum optical transmission in the silicon solar-cell sensitivity wavelength range of 0.4 to 1.1 μm.

(2) Retention of a required level of electrical insulation to protect against electrical breakdown, arcing, etc., with the associated hazards of electrical fires and other dangers to human safety.

(3) The mechanical properties to maintain spatial containment of the solar cells and interconnects, and to resist mechanical creep. The mechanical properties also must not impose undue mechanical stresses on the solar cell.

When exposed to outdoor weathering, polymeric materials can undergo degradation that could affect their optical, mechanical, and electrical insulation properties. Outdoors, polymeric materials can degrade from one or more of the following weathering actions (Reference 10):

(1) Ultraviolet (UV) photooxidation.

(2) UV photolysis.

(3) Thermal oxidation.

(4) Hydrolysis.

For expected temperature levels (References 9, 11, 12, and 13) in operating modules, up to 60°C in a rack-mounted array and possibly up to 80°C on a rooftop, three generic classes of transparent polymers are generally resistant to the above weathering actions: silicones, fluorocarbons, and polymethyl methacrylate (PMMA) acrylics. Of these three, only silicones, which are expensive, have been available as low-modulus elastomers suitable for pottant application.

Therefore, all other transparent, low-modulus elastomers will in general be sensitive to some degree of weathering degradation. However, less weatherable and lower-costing materials can be considered for pottant application if the module design can provide the necessary degree of environmental protection. For example, a hermetic design such as a glass superstrate with metal-foil back cover and appropriate edge sealing will essentially isolate the interior pottant from exposure to oxygen and water vapor, with the glass itself providing a level of UV shielding. As an illustration, polyvinyl butyral (PVB) would undergo rapid deterioration if directly exposed outdoors to oxygen, water vapor, and UV, but when isolated within the core of a double-glass automotive windshield, PVB lasts virtually forever. PVB is used as a lamination pottant in many commercial glass-superstrate PV modules.

The situation is different, however, for a substrate module that employs a weather-stable plastic-film front cover. Because all plastic films are permeable to oxygen and water vapor (Reference 14), the pottant is exposed to oxygen and water vapor, and also to UV if the plastic film is non-UV screening. Because isolation of the pottant from oxygen and water vapor is not practical in this design option, it becomes a requirement that the pottant be intrinsically resistant to hydrolysis and thermal oxidation at service temperatures, but sensitivity to UV is allowable if the weather-stable front-cover plastic film can provide UV shielding. (Commercial UV-screening plastics have been identified for this application, and are under study.)

Therefore surveys (Reference 3) were done to identify the lowest-costing, transparent, low-modulus elastomers with expected resistance to hydrolysis and thermal oxidation at temperatures up to 80°C, but these materials were allowed to be sensitive to UV deterioration. It was envisioned that if such a set of lowest-costing pottant candidates were selected on the basis of a less-protective substrate-module design, they would also be usable in a potentially more-protective glass-superstrate design.

In addition to the foregoing requirements for candidate pottant selection, these materials must also be capable of being fabricated into modules by industrial fabrication methods. Therefore, the materials must be readily usable on commercial equipment. The two industrial fabrication techniques in common use are lamination and casting.

The general plan for the FSA development of pottants encompasses two discrete steps:

(1) Evaluation Readiness: An intermediate stage of development wherein the material can be handled, processed, and fabricated into modules by participating industrial manufacturers. Although

fabricability using commercial equipment becomes the key criterion for this level of development, the material will be fully compounded with trial anticxidants, UV stabilizers, other necessary additives, and complete with recommended processing conditions and primers and adhesives.

(2) Application Readiness: The final stage of development in which the material will incorporate improvements in the intermediate-stage material generated by:

(a) Feedback on handling, processing, and fabricability of the intermediate-stage material by participating PV manufacturers.

(b) Results of accelerated, abbreviated, and outdoor testing of the material and of modules fabricated with the material.

The following list outlines some of the features of a pottant ready for application evaluation:

(1) Fastest possible fabrication cycle:

(a) Lowest possible cure temperature.

(b) Fastest possible cure time.

(2) Self-priming.

(3) Specification of peak-service temperatures for 20-yr life in various module designs (superstrate and substrate).

Although pottants may be developed to this stage by FSA, further refinements could be made by material or module manufacturers who may devise additional modifications.

Based on FSA pottant experience, certain specifications and requirements for pottants are emerging; these are shown in Table 1.

Ethylene vinyl acetate has been developed to the evaluation-ready stage, and is currently being advanced toward the application-ready stage. The evaluation-ready version of EVA is now commercially available. This document describes the development, properties, and status of the evaluation-ready version of EVA, and additionally reports on early efforts and preliminary results arising from activities related to application readiness. Table 2 is a master list of materials being evaluated experimentally for all module construction elements (Figure 2) by FSA. A description of each of these materials is reported in more detail in Reference 8.

Table 1. Evolving Specifications and Requirements for Compounded Pottant Materials

Characteristic	Specification or Requirement
Glass transition temperature (T_g)	$<-40^{\circ}C$
Total hemispherical light transmission through a 20-mil-thick film integrated over the wavelength range from 0.4 μm to 1.1 μm	>90% of incident
Hydrolysis	None at 80°C, 100% RH
Resistance to thermal oxidation	Stable up to 150°C
Mechanical creep	None at 90°C
Tensile modulus as measured by initial slope of stress-strain curve	<3000 lb/in.^{2} at 25°C
Fabrication temperature	$\leq 170^{\circ}C$ for either lamination or liquid pottant systems
Fabrication pressure for lamination pottants	≤ 1 atm
Chemical inertness	No reaction with embedded copper coupons at 90°C
UV absorption degradation	None at wavelength >0.35 μm
Hazing or clouding	None at 80°C, 100% RH
Minimum thickness on either side of solar cells in fabricated modules	6 mils
Odor, human hazards (toxicity)	None

Table 2. Candidate Encapsulation Materials Being Evaluated Experimentally by FSA

Function	Material	Type	Source
Low-Soiling Surface Material	Fluorinated silane	L-1668	3M
	Perfluorodecanoic acid	With E-3820 primer	Dow Corning
UV Screening Front Cover	Low-iron tempered float glass	E.g., Sunadex glass	ASG
	UV-screening acrylic films	Acrylar X-22416 2 mils thick	3M
		Acrylar X-22417 3 mils thick	3M
	UV-screening PVF fluorocarbon film	Tedlar 100 BG30UT 1 mil thick	Du Pont
Pottant	EVA	A-9918	Springborn, Du Pont, and Rowland, Inc. (Berlin, CT)
	Ethylene methyl acrylate (EMA)	A-11877	Springborn
	Poly-n-butyl acrylate (PnBA)	BA-13870	Springborn
	Polyurethane	Z-2591	Development Associates, North Kingston, R.I.
Porous Spacer	Craneglas non-woven E-glass material	Type 230, 5 mils thick	Electrolock, Inc. (Chagrin Falls, OH)
Dielectric Film	Candidates are the front and back cover plastic film		

Table 2. Candidate Encapsulation Materials Being Evaluated Experimentally by FSA (Cont'd)

Function	Material	Type	Source
Substrates	Mild steel	Cold-rolled	Various
	Hardboards	Super-Dorlux, 1/8 in. thick	Masonite
		Duron, 1/8 in. thick	U.S. Gypsum
Back Covers	White-pigmented plastic film	Tedlar 150 BL30WH, 1.5 mils thick	Du Pont
	White-pigmented plastic film	Tedlar 400 BS20WH, 4.0 mils thick	Du Pont
	White-pigmented plastic film	Scotchpar 10 CP White 1.0 mil thick	3M
	White-pigmented plastic film	Scotchpar 20 CP White 2.0 mils thick	3M
	White-pigmented plastic film	Korad 63000 White, 3.0 mils thick	Xcel Corp.
Edge Seal and Gasket	Butyl edge-sealing tape	5354	3M
	EPDM gasket-sealing tape	E-633	Pawling Rubber Co. (Pawling, NY)

SECTION III

ETHYLENE VINYL ACETATE, A LOW-COST POTTANT

A. HISTORICAL DEVELOPMENT

EVA is a copolymer of ethylene and vinyl acetate typically sold in pellet form by Du Pont Co. and U.S. Industrial Chemicals, Inc. (U.S.I.). The Du Pont trade name is Elvax; the U.S.I. trade names are Ultrathene and Vynathene. The cost of EVA typically ranges between $0.60 and $0.70 per lb (1980 dollars). All commercially available grades of EVA were evaluated, and four candidates, based on maximum optical transmission, were identified: Elvax 150, Elvax 250, Elvax 4320 and Elvax 4355 (Reference 3). Because EVA is thermoplastic, processing into a module is best accomplished by vacuum-bag lamination with a film of EVA. Based on film extrudability and transparency, the best choice became Elvax 150, at a cost (for high-volume purchases) of about $0.65/lb. Elvax 250 was a close second choice.

Elvax 150 softens to a viscous melt above 70°C, and therefore is not suitable for temperature service above 70°C when employed in a fabricated module. A peroxide cure system was developed for Elvax 150 that results in a temperature-stable elastomer (References 3 and 6); Elvax 150 was also compounded with an antioxidant and UV stabilizers, which improved its weather stability but did not affect its transparency.

In addition to clear EVA, a white-pigmented EVA film was formulated (with ZnO_2 and TiO_2) that can be positioned on the back side of the solar cells in a module layup. The pigment provides a light-reflecting background for those module areas not covered by solar cells and increases module power output by internal reflection.

The development of Elvax 150 toward evaluation readiness involved two trial compounding formulations. The first formulation became available in the fall of 1978, and several module manufactures evaluated it by fabricating modules using their own commercial solar cells. The processing technique in all cases was vacuum-bag lamination. The manufacturers reported certain advantages of EVA when compared to PVB, a laminating film material in common use within the PV module industry. The reported advantages were:

(1) Its cost is lower.

(2) Its appearance is better.

(3) It has better clarity.

(4) It obviates cold storage.

(5) It has dimensional stability.

(6) It has processing advantages:

(a) It requires less time.

(b) It obviates the use of a pressure autoclave.

(7) It has good flow properties and volumetric fill.

Continued experimentation with the first trial EVA formulation resulted in identification of a better antioxidant (Naugard-P) for Elvax 150, which is now used in the second formulation of EVA, and which is the evaluation-ready version (Reference 6). The formulations for the clear and white-pigmented evaluation-ready EVA films are listed in Table 3. These ingredients are compounded in Elvax 150 pellets, followed by extrusion at 85°C to form a continuous film. The thickness of the clear film is nominally 18 mils; the white-pigmented film is nominally 14 mils thick. The selected curing system is inactive below 100°C, so that film extruded at 85°C undergoes no curing reaction. The extruded film retains the basic thermoplasticity of the Elvax 150. Therefore, during vacuum-bag lamination, the material will soften and process as a conventional laminating resin. A complete description of the EVA curing properties and of the the EVA lamination process follows in the next section.

Clear EVA films of Springborn Laboratories, Inc., Formulation A-9918 are available from two sources: Rowland, Inc.*, and Springborn.

B. CURE AND PROCESSING

1. Cure

The EVA copolymer (Elvax 150, Du Pont) is cured with an aliphatic peroxide curing agent, Lupersol 101. This was selected because of its negligible decomposition and cure activity at 85°C to 90°C, the temperature range at which the EVA is extruded to a film. Trial experimentation (Reference 3) established that the Naugard-P antioxidant does not interfere with its curing properties at elevated temperatures, nor is the antioxidant consumed as a result of the peroxide curing reaction. Many candidate peroxide curing agents were eliminated (Reference 3) because of these detrimental interactions with the antioxidants.

Laboratory experiments with the Lupersol 101 peroxide curing agent established a time-temperature relationship for achieving acceptable and repeatable cure of EVA. The cure curve is shown in Figure 3. The criterion for acceptable cure was the achievement of mechanical-creep resistance of the cured EVA at 90°C, which corresponded to a gel content greater than 65%. The laboratory experiments involved very rapid heating of the A-9918 EVA to a specified cure temperature, typically in less than 1 min, followed by monitoring of the level of cure (gel content) as a function of cure time at constant temperature. Under these laboratory conditions, about 20 min at 150°C was required to achieve acceptable cure, and the required cure times were observed to increase by a factor of nearly three for every 12°C decrease in cure temperature, and vice versa. Laboratory experiments also

---

*Rowland, Inc.
Spruce Brook Industrial Park
Berlin CT 06037
(203) 828-6364

Table 3. Formulation of Evaluation-Ready Ethylene Vinyl Acetate

Ingredient	Function	Formulation, parts per hundred parts of Elvax 150	
		A-9918 Clear	A-9930B Pigmented
Elvax 150	Base EVA	100	100
Lupersol 101	Curing agent	1.5	1.5
Naugard-P	Antioxidant	0.2	-
Tinuvin 7709	UV stabilizers	0.1	-
Cyasorb UV-531	UV stabilizers	0.3	-
TiO_2	White pigments	-	2.0
ZnO_2	White pigments	-	5.0
Ferro AM-105	UV stabilizer	-	0.5

indicated that the Elvax 150 EVA copolymer could not be cured acceptably with Lupersol 101 below 120°C.

Volatile decomposition products generated by the thermal decomposition of the peroxide are prevented from forming permanent gas bubbles in the cured EVA by action of the lamination pressure. Laboratory experiments have adequately shown that 1 atm of lamination pressure at 150°C prevents the thermally decomposing peroxide from forming permanently trapped gas bubbles in the cured EVA. However, use of lamination pressures at less than 1 atm at 150°C may lead to insufficient containment pressure, resulting in trapped gas bubbles in the cured EVA. At lower pressure (<1 atm) lamination, this may be corrected by trial-and-error lowering of the peak cure temperature, but will also necessitate progressively longer cure times for the EVA to reach a minimum gel content of 65%.

A preliminary insight into the chemistry of the EVA/peroxide-curing mechanism is provided by a laboratory test (Reference 15) that involved curing, with Lupersol 101, a series of EVA resins varying in vinyl acetate content. Included in the series was a pure polyethylene, which for the purpose of this test was considered to be an EVA with zero wt % vinyl acetate. The cure results are shown in Table 4, which reveals that the cure reaction requires the vinyl acetate group; the pure polyethylene without vinyl acetate groups did not cure. Further, the efficiency of cure, as indicated by gel content, appears to be virtually independent of vinyl acetate content.

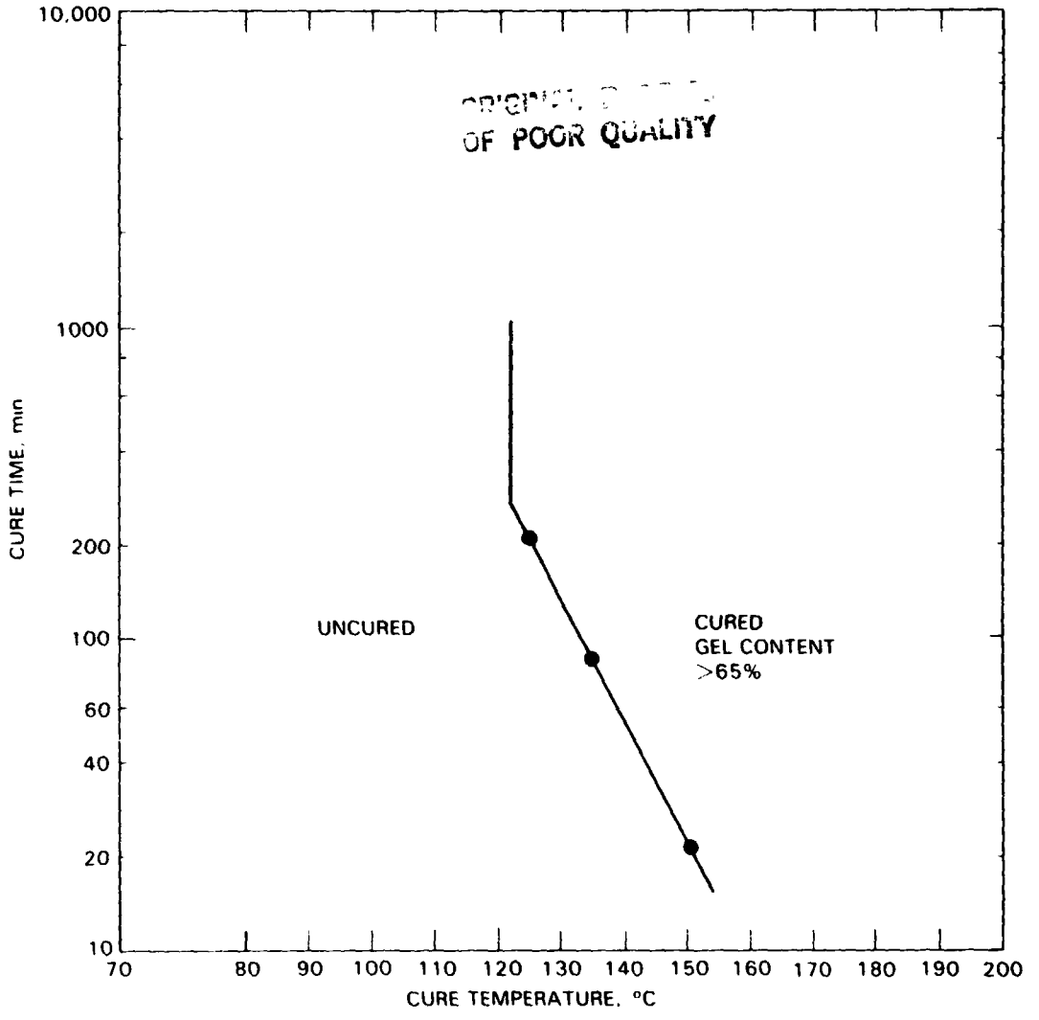

Figure 3. Laboratory-Measured Cure Conditions for Ethylene Vinyl Acetate Formulation No. A-9918

Exact details of the chemical curing reaction between the vinyl acetate groups and the peroxide have yet to be learned.

2. Processing

A successful and predictable module-fabrication process for EVA pottant has been achieved through a double vacuum-bag technique (Reference 7). To implement this technique, a special piece of equipment was built. The apparatus, schematically shown in Figure 4 and detailed in Figure 5, consists of a double-sectioned aluminum picture frame, closed at the top and bottom by aluminum plates. A flexible polymer diaphragm separates upper and lower cavities, and also function as a vacuum-tight gasket. Each chamber has its own vacuum gauges and valves for its individual evacuation. The top-cover plate is permanently attached and sealed to the top cavity with bolts and a

Table 4. Peroxide Curing of a Series of EVA Resins[a]

Resin	Vinyl Acetate, wt %	Gel Content, %
Elvax 150	33	75
UE-646-04	28	79
Elvax 240	28	71
Elvax 250	28	83
Elvax 350	25	73
Elvax 420	18	62
Elvax 450	18	86
Elvax 550	15	82
Elvax 650	12	66
Elvax 750	9	61
PE-831	0	0

[a]All polymers cured with 1.5 parts of Lupersol 101 per hundred parts of resin at 150°C for 20 min.

silicone rubber gasket. The lower plate is removable and seals to the bottom of the lower frame piece with a silicone-rubber O-ring gasket. The diaphragm material used is a high-temperature nylon film, 0.003 in. thick, which is flexible but not elastic. Conceivably, other types of films would work well in this application.

The module assembly is placed under the flexible diaphragm, in the lower cavity. The top surface of the module assembly is positioned flush with the top edge of the lower cavity, by stacking a necessary number of thin metal plates in the bottom of the lower cavity. The double vacuum-bag design enables initial exposure of the module assembly to a vacuum without simultaneous compression of the diaphragm, thus greatly enhancing air exhaustion from the module assembly. To ensure thorough air exhaustion, especially from large-area modules, the use of air-release scrim sheets of material such as Craneglas (Table 2 and Reference 8) should be incorporated in the module assembly. Experimentation has demonstrated that a 5-mil-thick Craneglas mat can be positioned above the active surface of the solar cells without optical obstruction (Reference 9).

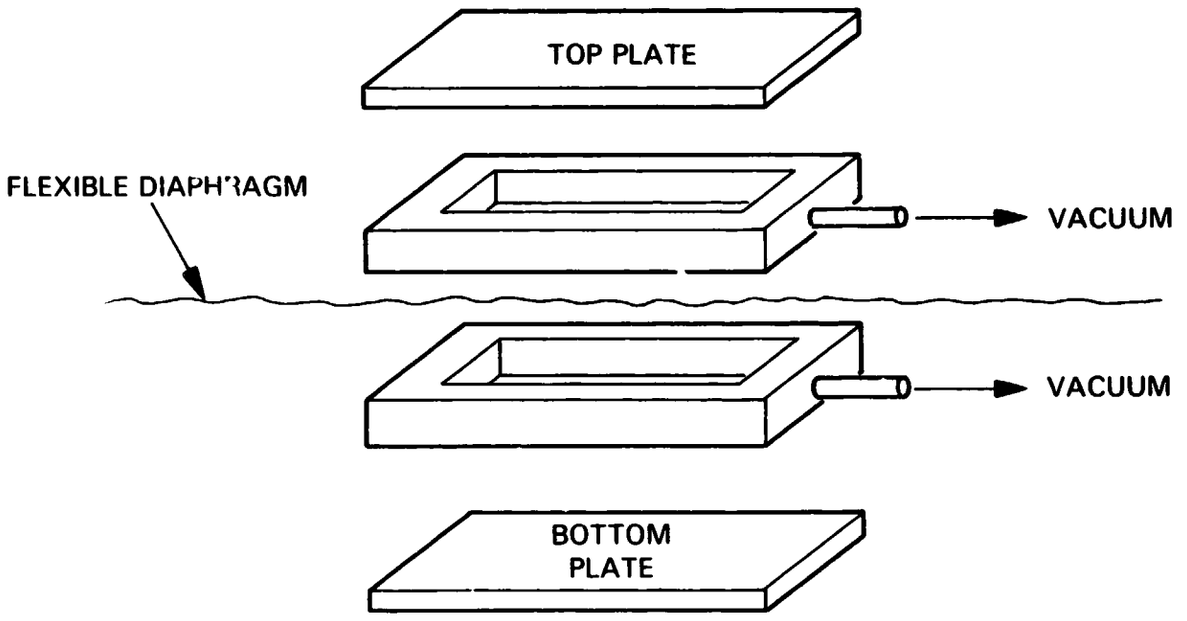

Figure 4. Double Vacuum-Bag Fixture

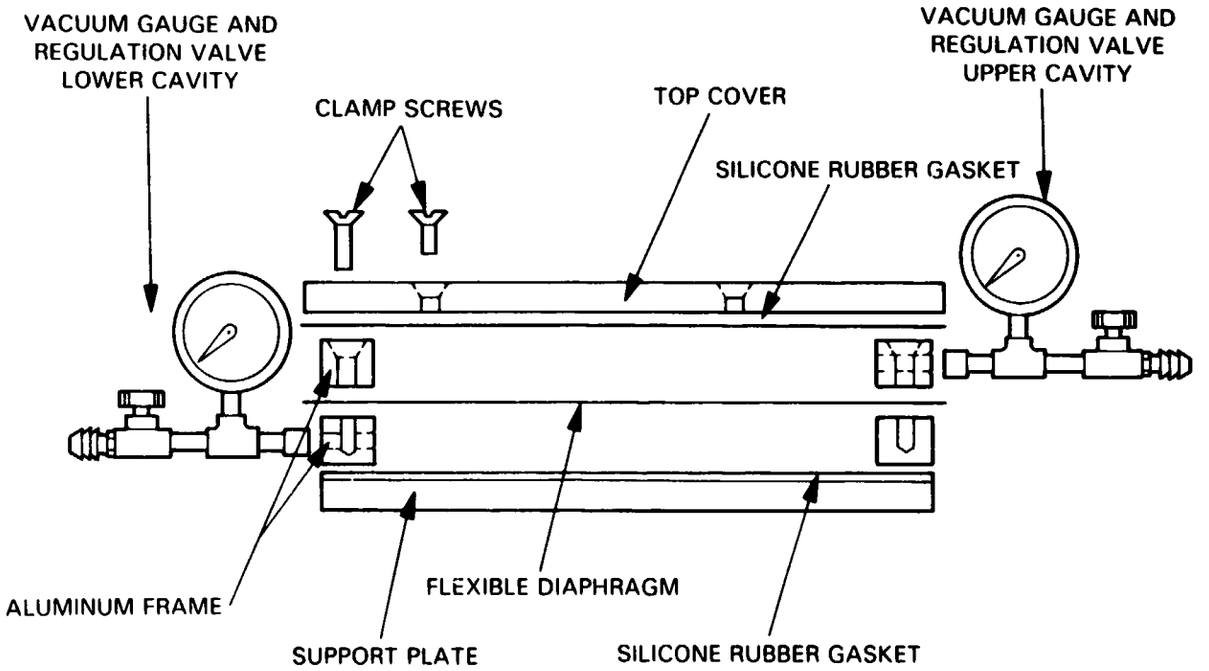

Figure 5. Experimental Double Vacuum-Bag Assembly

Diaphragm compression c. the module assembly can be done at any stage of the lamination cycle by pressurizing the upper cavity. Compression should be initiated or achieved, however, before the temperature of the EVA reaches 120°C.

In practice, t.e module components are preassembled into a sandwich before the encapsulation step. The basic assembly of materials required for vacuum-bag processing of substrate and superstrate modules are shown in Table 5.

Once the basic module components for either design have been assembled, a 10-mil-thick fluorinated ethylene propylene (FEP) release film or an equivalent should be included above and below the assembly. The release films should be cut to match the area of the module. These outer FEP film layers are then taped together over the edges of the module assembly with masking tape to contain the EVA when it softens during the heating cycles. The wrap-around of masking tape is attached to the FEP film layers, rather than to surfaces of the module. Although the edges are taped firmly, entrapped air seems to diffuse out easily. Innovation in equipment design will probably eliminate this taping procedure.

A useful fabrication aid is to include two 5-mil-thick (or thicker) metal (steel or aluminum) plates, one on each side of the taped module assembly. These plates distribute the lamination pressure over the module area, and result in uniformly thick modules, with smooth, wrinkle-free back-cover or front-cover surfaces.

The completed module assembly with taped edges is then placed in the lower cavity of the laminator and a microthermocouple is taped onto the FEP release film at the module center. The thermocouple permits convenient monitoring of the module temperature during the lamination cycle. The flexible diaphragm and upper-cavity fixtures are then positioned.

Both the upper and lower cavity are evacuated at room temperature for 5 to 10 min before heating, to exhaust the air from within the module assembly. While maintaining continuous vacuum in both the upper and lower cavity, the entire vacuum-bag fixture is loaded between the preheated (150°C) platens of a hydraulic press (Figure 6), which serve as the heat source. The ram pressure is just sufficient to close the press and provide good heat transfer to the vacuum-bag fixture. The pressure from the platen should rest only on the frame of the fixture and should not contribute any pressure to the surface of the module.

The time-temperature heating pattern of the module assembly after loading the vacuum-bag fixture into the preheated hydraulic press is shown in Figure 7. Experimentation with this heating process has demonstrated that a dwell time of 10 min at 150°C results in an acceptable EVA cure (less than the 20 min determined in the laboratory testing). The reduced dwell time reflects the degree of partial curing that occurs during the heat-up time to 150°C (faster or slower heating rates may require adjustment of the dwell time at the peak cure temperature). Samples of EVA taken from modules laminated by this process and associated time-temperature heating patterns exhibit acceptable cure with gel content over 75%.

Table 5. Basic Assembly of Materials Required for Vacuum-Bag Processing of Substrate and Superstrate Modules[a]

Superstrate[b]		Substrate[b]	
Material	Function	Material	Function
White plastic film	Back cover	Clear plastic film	UV-screening front cover
Clear EVA	Transparent pottant	Clear EVA	Transparent pottant
Craneglas	Air release mat		
(Solar Cells with Interconnects, Face Down)		(Solar Cells with Interconnects, Face Up)	
Clear EVA	Transparent pottant	Craneglas	Air release mat
Craneglas	Air release mat	White EVA	For light-reflecting background
Glass, primed[c]	Superstrate	Substrate	Substrate

[a]From top to bottom, as assembled.
[b]These two basic designs have been fabricated with success. The clear EVA is 0.018 in. thick. The load-bearing member, either superstrate or substrate, always faces the bottom of the assembly.
[c]The EVA primer is described in Table 6.

In this process, pressurization of the upper cavity to 1 atm of pressure is initiated when the module assembly temperature reaches 120°C. A slow pressurization scheme is not mandatory nor necessarily optimal, and users of EVA material may explore alternative pressurization techniques. The double-vacuum-bag fixture provides a capability of limiting pressurization in the upper cavity to less than 1 atm. However, low-pressure (<1 atm) lamination has not yet been experimentally investigated to determine the effect of pressure in inhibiting gas-bubbles formation due to peroxide decomposition.

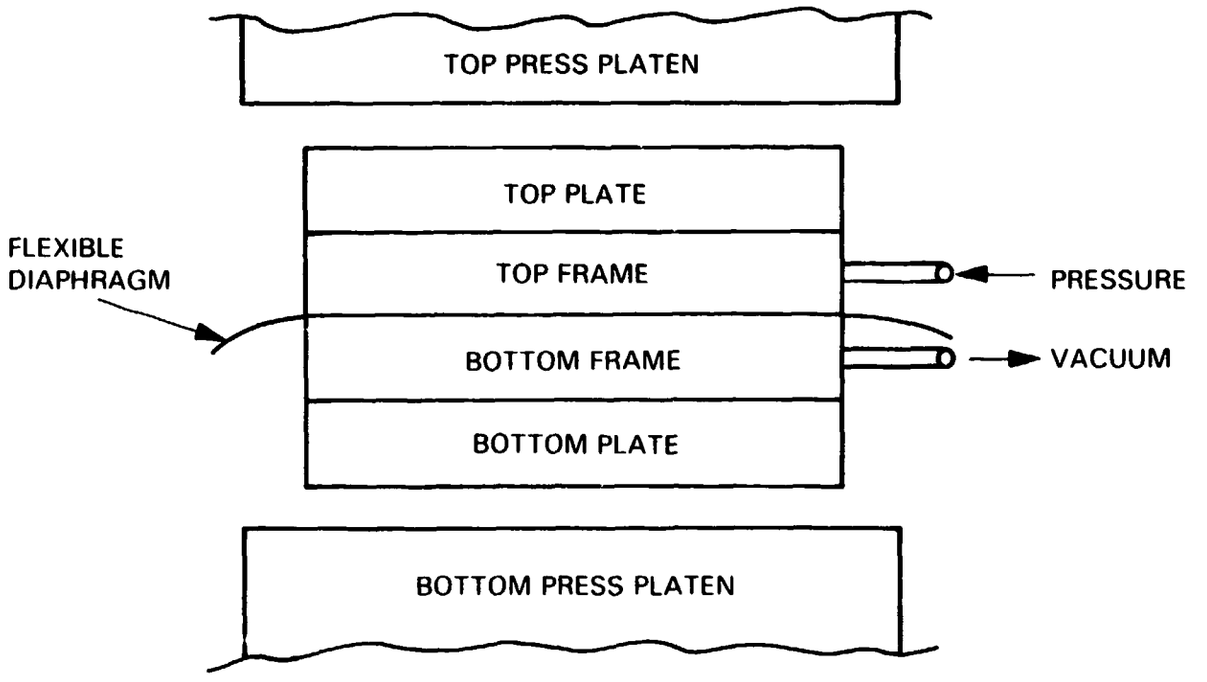

Figure 6. Vacuum-Bag Fixture Heated in Hydraulic Press

After the 10-min dwell at 150°C, the laminator can be removed from the heating press and permitted to cool in still air. When a temperature of about 40°C is reached, the vacuum in the lower cavity may be released, and the completed module may be removed from the laminator.

Modules prepared by the proceding process have been fully cured, and are bubble-free and of good appearance. No evidence of cell damage has been noticed.

Laboratory testing has not been done to investigate the effects on cure, if any, of the rate of temperature increase that the module assembly experiences during heating. The average EVA heating rate in this process is about 4°C/min.

The laboratory process described above evolved from efforts to achieve EVA module fabrication by a fast, reproducible process that would not damage solar cells nor incorporate bubbles, voids, or other defects that could be nuclei for module failure or problems. During the development of the EVA lamination process, two problems of significance, trapped bubbles and failure of the EVA to cure, were encountered, which necessitated detailed studies (References 3 and 4) of EVA cure technology and an understanding of the origin and elimination of trapped bubbles (i.e., two sources: trapped air, and volatiles from peroxide decomposition).

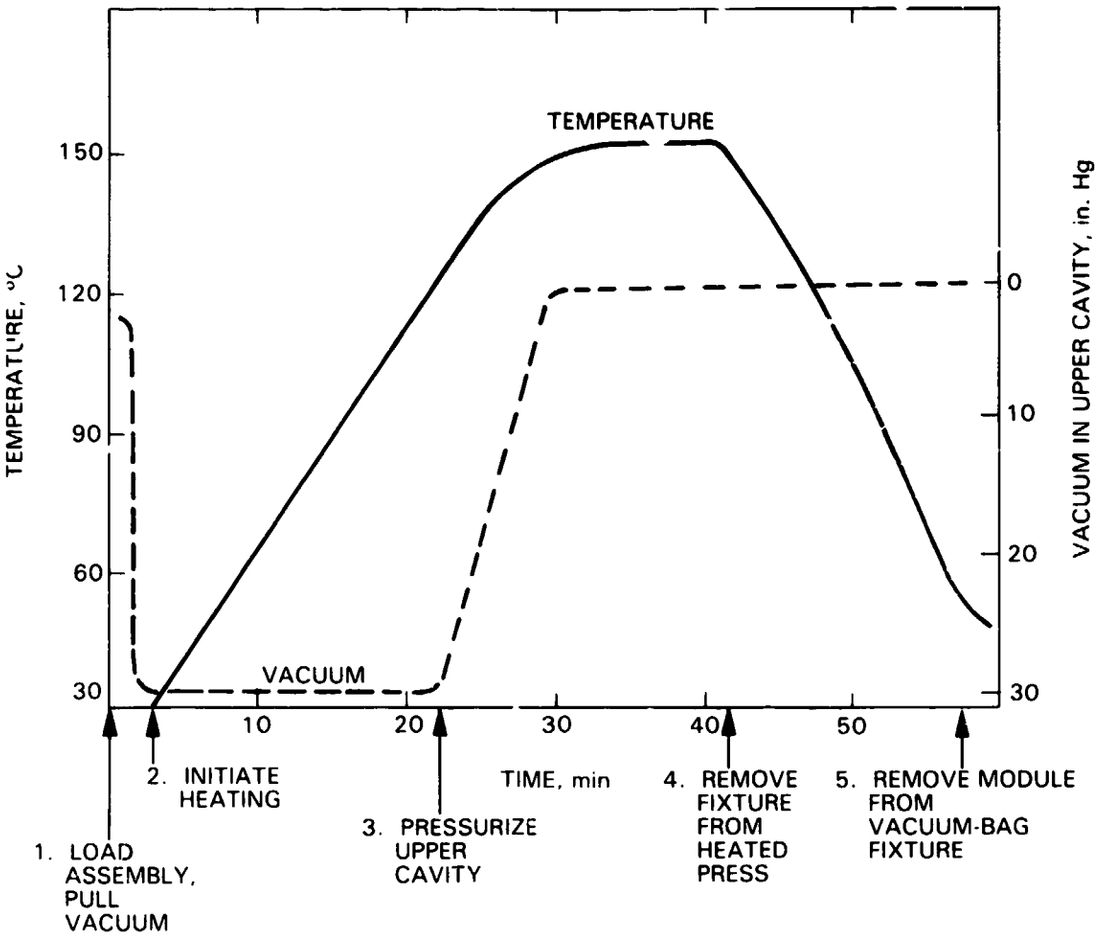

STEPS:

1. LOAD PREASSEMBLED MODULE INTO VACUUM-BAG FIXTURE AND PUMP BOTH CAVITIES DOWN TO 30 in. Hg FOR AT LEAST 5 min.
2. LOAD FIXTURE INTO PREHEATED PLATEN PRESS TO HEAT AT APPROXIMATE RATE OF 4°C/min BOTH CAVITIES ARE KEPT UNDER FULL VACUUM.
3. AT A TEMPERATURE OF 120°C, THE PRESSURE OF THE UPPER CAVITY IS GRADUALLY INCREASED TO ROOM PRESSURE OVER AN 8 TO 10-min PERIOD.
4. THE FIXTURE IS LEFT IN THE PRESS FOR 10 min AFTER REACHING A TEMPERATURE OF 150°C, THEN REMOVED WITH THE LOWER CAVITY STILL UNDER VACUUM.
5. THE MODULE CAN BE REMOVED FROM THE VACUUM-BAG FIXTURE AFTER COOLING FOR ABOUT 10 TO 15 min.

Figure 7. Module Fabrication: Temperature-Pressure Schedule

Table 6. Properties[a] of Elvax 150 and Cured A-9918 EVA

Property	Condition	Elvax 150	A-9918 EVA	Remarks
Optical Transmission		90.5%	91.0%	ASTM E-424 (Springborn)
Glass Transition Temperature, T_g		-43°C	-43°C	JPL measurement
Young's Modulus[b]	23°C	850 lb/in.^{2}	890 lb/in.^{2}	ASTM D-638 (Springborn)
	23°C	700 lb/in.^{2}	-	ASTM D-1708 (Du Pont)
Secant Modulus	1% elongation, 23°C	-	1120-1330 lb/in.^{2}	ASTM D-882 (Du Pont)
Tensile Strength at Break	23°C	850 lb/in.^{2}	1890 lb/in.^{2}	ASTM D-638 (Springborn)
	23°C	700-900 lb/in.^{2}*	1160-1490 lb/in.^{2}**	ASTM D-638*/D-882** (Du Pont)
	23°C	850 lb/in.^{2}	-	ASTM D-1708 (Du Pont)
	-20°C	2700 lb/in.^{2}	-	ASTM D-638 (Du Pont)
Elongation at Break	23°C	1050%	510%	ASTM D-638 (Springborn)
	23°C	900%-950%*	580 - 740%**	ASTM D-638*/D-882** (Du Pont)
	23°C	1050%	-	ASTM D-1708 (Du Pont)
	-20°C	300%	-	ASTM D-638 (Du Pont)
Flexural Modulus	23°C	1000 lb/in.^{2}	-	ASTM D-790 (Du Pont)
Compression Modulus	10 days at 25°C	65%	-	ASTM D-395 (Du Pont)
	22 h at 70°C	91%	-	ASTM D-395 (Du Pont)
Stiffness	23°C	800 lb/in.^{2}	-	ASTM D-747 (Du Pont)
	-20°C	4300 lb/in.^{2}	-	ASTM D-747 (Du Pont)
Hardness	Shore A, 10s	65-73	76-79	ASTM D-2240 (Du Pont; Springborn)
	Shore D, 10s	24	-	ASTM D-2240 (Du Pont)
Vinyl Acetate Content		33 wt %	33 wt %	Du Pont technical bulletins
Density, g/cm^3	23°C	0.957*	0.920**	Du Pont*/JPL** measurements
Refractive Index, n_d	25°C	1.482*	1.482**	Du Pont*/Springborn** measurements
Dielectric Strength, V/mil	25°C	-	620	Spectrolab measurement
	25°C	-	580	Springborn measurement
Water Absorption	23°C, 24 h water immersion	0.13 wt %	-	ASTM D-570 (Du Pont)
	18-a Film, 55°C, 100% RH	-	0.70 wt %	16-h exposure (JPL)
Specific Heat, W-s/g-°C		-	2.09	Spectrolab measurement
Thermal Conductivity, W-mil/ft^2-°C		-	9 x 10^2	Spectrolab measurement
Infra-Red Emissivity	25°C	-	0.88	JPL measurement
Thermal Expansion	Below T_g(-43°C)	1.0 x 10^{-4} °C^{-1}	0.9 x 10^{-4} °C^{-1}	JPL measurement
	-43°C to +10°C	-	2.0 x 10^{-4} °C^{-1}	JPL measurement
	Above +10°C	-	4.0 x 10^{-4} °C^{-1}	JPL measurement

[a]Sources: Property measurements made at Springborn Laboratories under FSA Contract No. 954527
Property measurements made at Spectrolab Inc. under FSA Contract No. 955567
Property measurements made at the JPL's analytical test facilities
Various Du Pont Technical Bulletins on Elvax resins
Du Pont Technical Bulletin "Elvax 150 Resin as a Solar Photovoltaic Module Pottant, Technical Guide," Polymer Products Department, Technical Services Laboratory, Wilmington, Delaware (June 1982).

[b]Initial slope of stress-strain curve

*, **: For each, refer to the Remarks column

Lessons learned from the laboratory development indicate that an industrial-scale EVA lamination method must:

(1) Prevent exposure of the EVA during heating to atmospheric oxygen, which was found to interfere chemically with the cure.

(2) Hold the module components physically in place (above 70°C, and before cure above 120°C to a tough elastomer, the EVA is in a fluid state).

(3) Apply uniform pressure over the surface area of the module during processing.

(4) Maintain constant vacuum for air and gas removal.

(5) Use air-release spacers (e.g., Craneglas) in the module assembly to facilitate total air removal from module interfaces.

The degree of cure (gel content) of the EVA may be determined by a simple laboratory procedure:

(1) Remove a small piece of cured EVA (1 to 2 g) and weigh on an analytical balance to three decimal places.

(2) Place the specimen in 100 ml of toluene and heat to 60°C for 3 hours.

(3) Pour the mixture through a piece of weighed filter paper to catch the gel fraction and permit it to drain completely.

(4) Dry the filter paper and gel fraction at 60°C for 3 to 4 hours (no odor of toluene solvent should remain).

(5) Weigh to three decimal places and subtract the weight of the filter paper.

(6) The gel content is calculated as:

$$\% \text{ gel} = \frac{\text{weight of EVA residue from toluene}}{\text{weight of original EVA specimen}}$$

(7) EVA with gel content over 65% may be regarded as acceptably cured. The described laboratory lamination process has resulted in gel content consistently ranging from 75% to 80%.

C. MATERIAL PROPERTIES

A data base of material properties of cured A-9918 EVA is emerging as the material is more intensively studied. Accumulated data on material properties are compiled in Table 6, along with material properties of the uncured and uncompounded Elvax 150, for comparison. The quoted properties for cured A-9918 EVA have been accumulated over time as needs arose for various

FSA contractors and JPL in-house studies, and in general are distributed throughout a plethora of contractor and JPL documents, and in a recently published Du Pont technical bulletin. The primary sources are listed in the footnote of Table 6. The properties of Elvax 150 are extracted from Du Pont technical bulletins for that product.

The major effects of crosslinking Elvax 150 are an increase in tensile strength and hardness, and a decrease in elongation-at-break and in density (Table 6). There is a slight increase in optical transmission and Young's modulus. All other properties measured in common are essentially unaffected by crosslinking. Figure 8 is a plot of the optical transmission of cured A-9918 EVA over the wavelength region from 390 nm to 1105 nm, as reproduced from a Du Pont technical bulletin.

The dynamic mechanical properties of uncured Elvax 150 and cured A-9918 EVA were measured at 110 Hz on a Rheovibron-dynamic test machine. Dynamic modulus and loss tangent as a function of temperature are plotted in Figures 9 and 10, respectively. The melting of uncured Elvax 150 to a fluid state is observed (Figure 9) to occur around 75°C to 80°C. After curing, the melting of Elvax 150 is prevented (Figure 9). The property of Elvax 150 of becoming fluid at 75°C to 80°C is why it is important to ensure adequate EVA cure. Without it, EVA in a module application would liquefy and flow at temperatures above 75°C to 80°C.

Tables 7 and 8 are water-related properties of EVA resins reproduced from technical bulletins for those products. Table 7 is a tabulation of water-absorption values of four EVA resins varying in vinyl acetate content, including Elvax 150. In general it is observed that water absorption decreases with decreasing vinyl acetate content. Table 8 is a tabulation of water-vapor-transmission rates for four EVA resins, over a resin density range from 0.930 to 0.945 g/cm^3. Since resin density increases with increasing vinyl acetate content (see Table 7 and Figure 11), these data indicate that water-vapor-transmission rates increase with increasing vinyl acetate content. The data could be extrapolated to a resin density of 0.957 g/cm^3 which is the density of Elvax 150, and therefore an estimate of water-vapor transmission rates for that material could be made.

D. CHEMICAL STRUCTURE OF ELVAX 150 EVA

This section describes a speculation on the chemical structure of Elvax 150 EVA. A fundamental understanding of its chemical structure can aid in the interpretation of the behavior of material properties that can result from crosslinking and outdoor weathering, and in the selection of potentially more effective anti-oxidants and UV stabilization additives.

EVA resins are reported (Reference 16) to be semicrystalline polymers, with the level of crystallinity being related to the vinyl acetate content. This same reference reports that at and above about 45 wt % vinyl acetate content, the EVA copolymers become completely amorphous. Elvax 150 with a vinyl acetate content of 33 wt % (Table 6) is therefore semicrystalline, and it is speculated that crosslinking of the Elvax 150 disrupts the crystallinity, resulting in either a completely amorphous copolymer or one with substantially reduced crystallinity content.

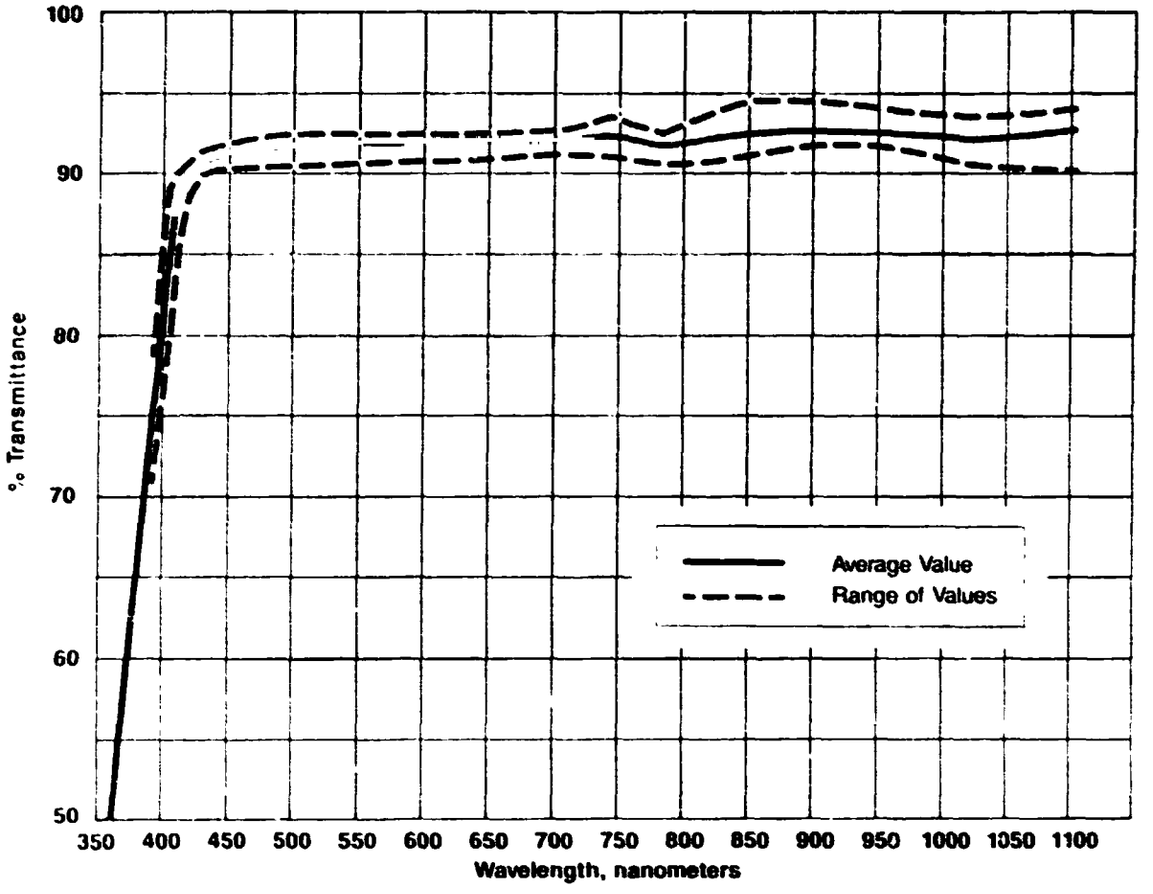

Figure 8. Average Solar Transmittance of Cured EVA A-9918 (390-1105 nm)*

Evidence for this speculation is found to a lesser extent in the slight increase in optical transmission of cured Elvax 150, but is found primarily in the substantial reduction in density, from 0.957 g/cm^3 to 0.920 g/cm^3. Ordinarily, elastomeric and rubbery materials experience a slight increase in density when crosslinked (Reference 17), but Elvax 150's density decreased when crosslinked. It is believed that the density reduction results from the elimination or reduction of crystallinity when the Elvax 150 is crosslinked.

This observation of a reduction in the density of Elvax 150 upon crosslinking also enables a further speculation about the chemical structure of EVA copolymer resins. Figure 11 is a plot of the room-temperature densities of Elvax EVA resins versus wt% vinyl acetate content, as extracted from Du Pont technical bulletins for Elvax products. The essentially linear plot extrapolates to a density near 0.92 g/cm^3 at 0 wt% vinyl acetate content, which is coincidental, but is not the explanation for the same density value acquired by the crosslinked Elvax 150. As described below, the extrapolated density

*Reproduced from Du Pont Technical Bulletin "Elvax 150 Resin as a Solar Photovoltaic Module Pottant, Technical Guide," Polymer Products Department, Technical Services Laboratory, Wilmington, Delaware, June 1982.

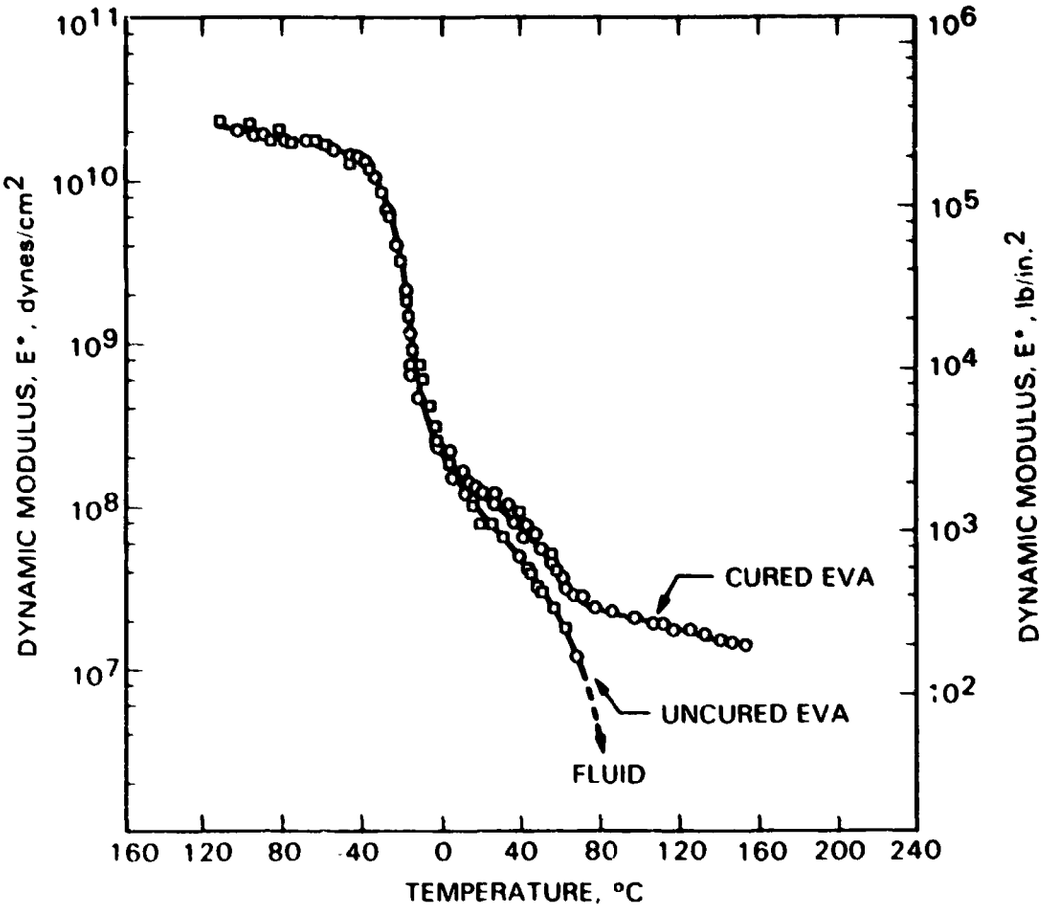

Figure 9. Dynamic Modulus (E) of Ethylene Vinyl Acetate A-9918 at a Frequency of 110 Hz

value of near 0.92 g/cm^3 in this speculation is to be associated with medium-density semicrystalline polyethylene. Further, the density plot of Figure 11 when extrapolated linearly to 100% vinyl acetate does not predict a density of 1.19, which is that of pure polyvinyl acetate at room temperatures.

But the density plot of Figure 11, and the density reduction after having cured Elvax 150, can be explained if it is assumed that EVA copolymer resins are block copolymers, having one block which is an amorphous, random copolymer of ethylene and vinyl acetate, and the other block being all semicrystalline polyethylene without any vinyl acetate component. An illustration of this speculative block copolymer structure is shown in Figure 12. With this block copolymer structure, the densities of the separate blocks can be estimated, followed by calculation of the density of the uncured resin and the reduced density of the cured EVA resin, for comparison with the known values.

The density calculations will be carried out for Elvax 150, which has a composition of 67 wt % ethylene and 33 wt % vinyl acetate. The density of a block copolymer can be estimated from the following equation:

$$\rho_p = W_{B1}\rho_{B1} + W_{B2}\rho_{B2} \qquad (1)$$

Table 7. Water Absorption[a] of Various Du Pont Ethylene Vinyl Acetate (Elvax) Resins[b]

Elvax Resin	Density, g/cm^3	Vinyl Acetate Content, %	Water Content, wt %
Elvax 150	0.957	33	0.13
Elvax 260	0.955	28	0.13
Elvax 360	0.950	25	0.11
Elvax 460	0.941	18	0.07

[a]ASTM D-570, 24-h water immersion at 23°C
[b]Source: Du Pont technical bulletins for Elvax EVA resins

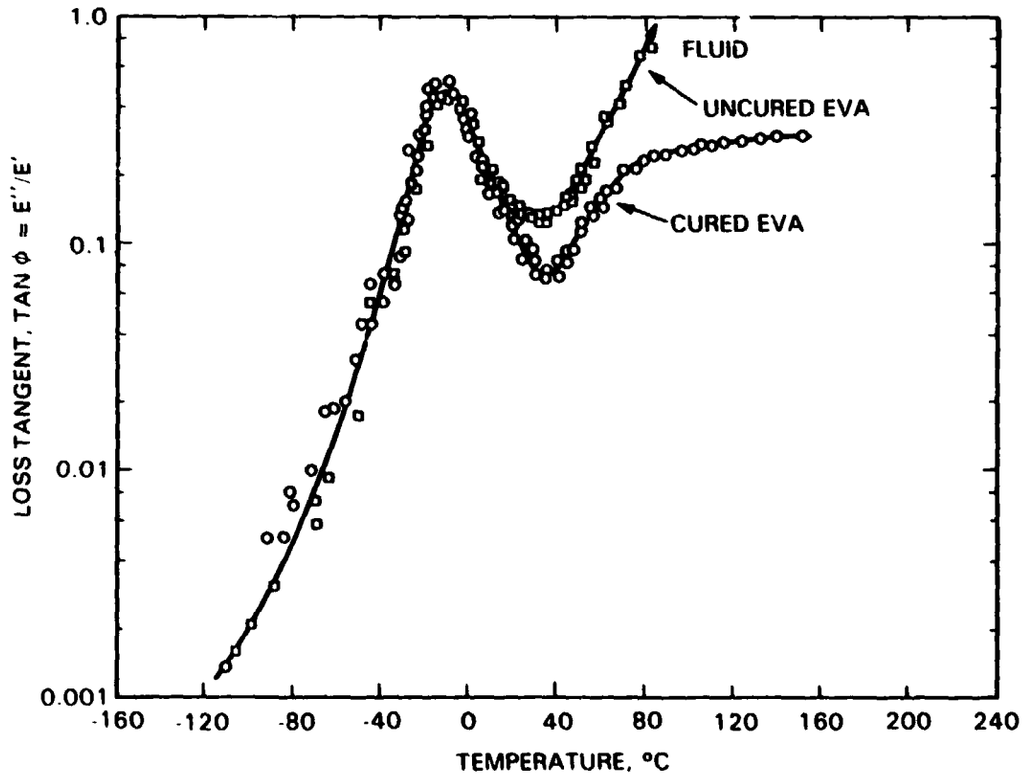

Figure 10. Loss Tangent (Tan ϕ) of Ethylene Vinyl Acetate A-9918 at a Frequency of 110 Hz

Table 8. Water-Vapor Transmission Rates (WVTR) of Ethylene Vinyl Acetate Resins[a]

$$\text{WVTR in units of } \frac{(\text{g } H_2O)\ (\text{mils})}{(\text{in.}^2)\ (\text{h})\ (\text{mm Hg})}$$

Resin Density, g/cm^3	WVTR at 20°C	WVTR at 38°C
0.930	1.75×10^{-5}	2.79×10^{-5}
0.935	3.40×10^{-5}	5.23×10^{-5}
0.940	5.33×10^{-5}	7.63×10^{-5}
0.945	7.14×10^{-5}	10.16×10^{-5}

[a]Source: U.S.I. Chemicals Technical Bulletin for Ultrathene EVA Copolymers, Fourth Edition (1972).

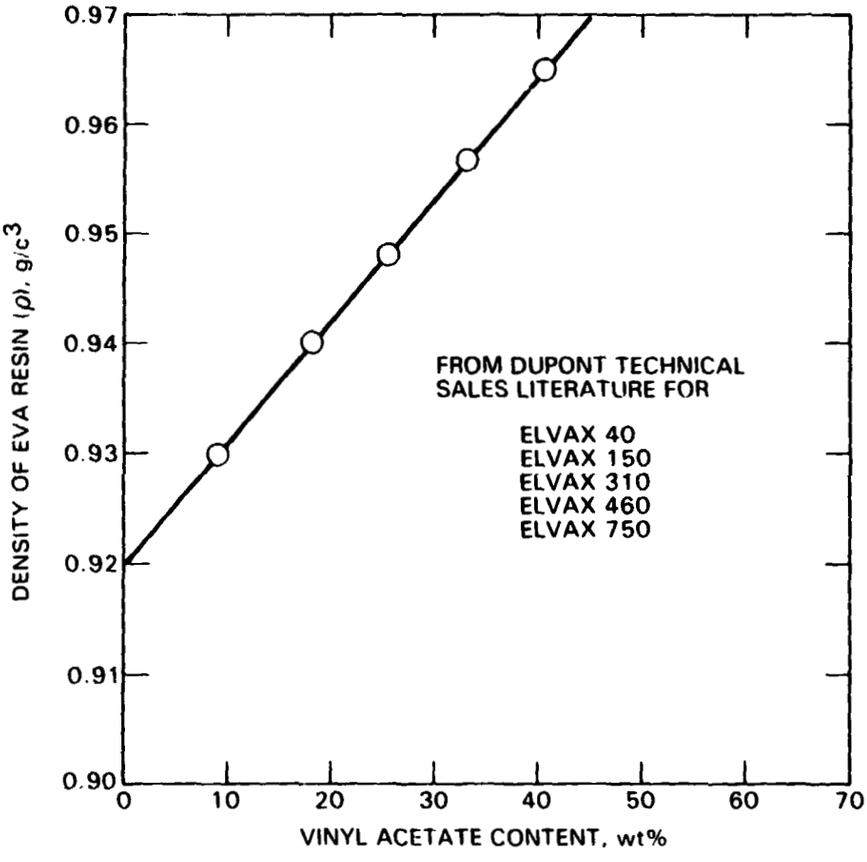

Figure 11. Densities of Elvax EVA Resins versus Vinyl Acetate Content

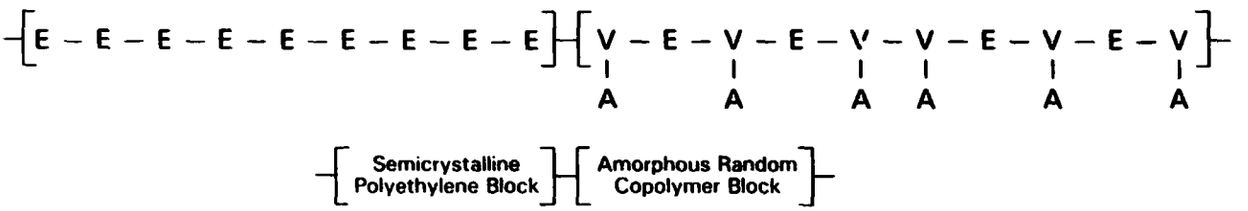

Figure 12. Speculations on the Polymeric Structure of Elvax 150 EVA: Block Copolymer

where

ρ_p = density of the block copolymer

ρ_{B1} and ρ_{B2} = densities of Block 1 and Block 2

W_{B1} and W_{B2} = weight fraction of Block 1 and Block 2

The density of a random copolymer can be estimated from the following equation:

$$\rho_c = M_1\rho_1 + M_2\rho_2 \qquad (2)$$

where

ρ_c = density of the random copolymer

ρ_1 and ρ_2 = densities of components 1 and 2

M_1 and M_2 = mol fractions of components 1 and 2

The density of amorphous polyethylene, which is assumed to be its physical state in the amorphous and random copolymer block, is 0.885 g/cm^3 (Reference 18). Further, all of the vinyl acetate in the Elvax 150 resin is assumed to be in the copolymer block, and none in the semicrystalline polyethylene block. Last, and because of the extrapolation of Figure 11 to a density of 0.92 g/cm^3 for 0 wt % vinyl acetate, it is assumed that this is the density P_{B1} of the semicrystalline polyethylene block. With this information, and the density and composition of Elvax 150, there are sufficient data to solve Equations (1) and (2) simultaneously for all of the unknowns. The given data and the calculated unknowns are tabulated in Table 9.

These results indicate that the polyethylene block of Elvax 150 is 53 wt % of the total resin, and the amorphous ethylene vinyl acetate block is 47 wt % of the total resin. In turn, the composition of the amorphous ethylene/vinyl acetate block is 70 wt % vinyl acetate and 30 wt % ethylene, or 43 mol % vinyl acetate and 57 mol % ethylene. The density ρ_c of the amorphous ethylene/vinyl acetate block is 1.00 g/cm^3. The total ethylene content distributed between the two blocks is 67 wt % of the Elvax 150, and the vinyl acetate content found only in the amorphous block is 33 wt % of the Elvax 150, which was given as a known.

Table 9. Composition of Elvax 150 When Assumed to be a Block Copolymer as Depicted in Figure 12

A.	INPUT DATA	
	1. Elvax 150	-- Density, ρ_p = 0.957 g/cm^3 -- Components = 67 wt % polyethylene, 33 wt % vinyl acetate
	2. Polyvinyl Acetate	-- Density, ρ_1 = 1.19 g/cm^3 -- Mol wt = 86 -- T_g = 29°C (302°K)
	3. Polyethylene	-- Amorphous density, ρ_2 = 0.885 g/cm^3 -- Mol wt = 28 -- T_g = 125°C (148°K)
B.	CALCULATED VALUES	
	1. Polyethylene Block	-- Density, ρ_{B1} = 0.92 g/cm^3 -- Wt fraction of resin, W_{B1} = 0.53 -- Mol wt ≈ 2500
	2. Ethylene/Vinyl Acetate Copolymer Block	-- Density, $\rho_C = \rho_{B2}$ = 1.00 g/cm^3 -- Wt fraction of resin, W_{B2} = 0.47 -- Mol wt ≈ 2250
	a. Copolymer Block Composition (mol fraction):	
	Vinyl acetate:	M_1 = 0.43
	Ethylene:	M_2 = 0.57
	b. Copolymer Block Composition (wt fraction):	
	Vinyl acetate:	X_1 = 0.70
	Ethylene:	X_2 = 0.30

Numerically the equation for the density ρ_c of the random and amorphous ethylene vinyl acetate block is

$$\rho_c = (0.43)\ (1.19) + (0.57)\ (0.885) = 1.00\ g/cm^3 \qquad (3)$$

and numerically the equation for the Elvax 150 resin density ρ_p is

$$\rho_p = (0.47)\ (1.00) + (0.53)\ (0.92) = 0.957\ g/cm^3 \qquad (4)$$

It was speculated above that the crosslinking of Elvax 150 reduces or eliminates crystallinity, as reflected in the reduction of the polymer density from 0.957 g/cm^3 to 0.92 g/cm^3. Since all of the polymer crystallinity is in the polyethylene block, and if it can be assumed that this block is rendered amorphous as a result of the steric disruption associated with crosslinking, then the density of the cured Elvax 150 can be calculated using Equation (1), using a density of 0.885 g/cm^3 for the resultant amorphous polyethylene block. Substituting a value of 0.885 for 0.92 in Equation (4) yields

$$\rho_p = (0.47)\ (1.00) + (0.53)\ (0.885) = 0.92\ g/cm^3 \qquad (5)$$

This calculated value of 0.92 g/cm^3 matches the measured density value for the crosslinked Elvax 150.

The essentially linear relationship between density and vinyl acetate content (Figure 11) can provide another speculation about the general copolymer characteristics of Elvax EVA resins, if it can be assumed that they all contain a semicrystalline polyethylene block of density 0.92 g/cm^3. Equation (1) can be rearranged to the following form:

$$\rho_p = \frac{V}{X_1} (\rho_{B2} - 0.92) + 0.92 \qquad (6)$$

where

ρ_{B2} = density of the amorphous ethylene/vinyl acetate block

V = vinyl acetate content in the total resin, wt %

X_1 = vinyl acetate content in the amorphous ethylene/vinyl acetate block, wt %

and 0.92 is the density of the semicrystalline polyethylene block. Equation (6) states that for constant X_1, and therefore also for constant ρ_{B2}, a straight-line relationship between ρ_p and V is predicted, with an intercept at V = 0 of 0.92.

Up to 40 wt % vinyl acetate content, a straight-line relationship, is observed in Figure 11, which suggests for these Elvax EVA resins that the composition of the ethylene/vinyl acetate block in all these resins is essentially constant at 70 wt % vinyl acetate and 30 wt % ethylene, and that therefore the vinyl acetate content V, based on the total resin, is regulated by variations in the weight-fraction mix of the two blocks.

The glass transition temperature (T_g) of random copolymers can be estimated with the following equation (Reference 19):

$$\frac{1}{T_g} = \frac{W_1}{T_{g1}} + \frac{W_2}{T_{g2}} \qquad (7)$$

where

T_g = glass transition temperature of the copolymer, °K

T_{g1} and T_{g2} = glass transition temperatures of components 1 and 2

W_1 and W_2 = weight fraction of components 1 and 2 in the copolymer

If it is assumed that Elvax 150 is indeed a random copolymer of ethylene and vinyl acetate rather than a block copolymer, as described above, its estimated T_g using Equation (7) is -95°C (178°K):

$$\frac{1}{T_g} = \frac{0.67}{148} + \frac{0.33}{302}; \; T_g = -95^{\circ}C \; (178^{\circ}K) \qquad (8)$$

where, in Equation (8), 0.67 and 148 are respectively the weight fraction of polyethylene in Elvax 150 and its T_g in ^oK, and 0.33 and 302 are respectively the weight fraction of polyvinyl acetate in Elvax 150 and its T_g in ^oK. Examination of the dynamic mechanical property curves (Figures 9 and 10) reveals no evidence of any transition event at or near -95°C. On the other hand, if a block copolymer structure is assumed, then two glass transition events would be expected, one for the polyethylene block and another for the amorphous, random-copolymer ethylene vinyl acetate block. Using Equation (7), the glass transition temperature of the amorphous, random-copolymer block can be estimated as follows:

$$\frac{1}{T_g} = \frac{0.3}{148} + \frac{0.7}{302}; \; T_g = -43^oC \; (230^oK) \qquad (9)$$

where 0.3 and 0.7 are respectively the weight fractions of ethylene and of vinyl acetate in the block. The estimated T_g of -43°C matches the temperature associated with a major glass transition temperature event observed in the dynamic mechanical property curves. Evidence for the glass transition temperature of the polyethylene block, -125°C, is not observed in the dynamic mechanical property curves, as the starting test temperature for these data measurements, unfortunately, was -115°C. In general, however, it is known that the glass transition temperature of polyethylene is not readily identifiable from dynamic testing (Reference 20).

Elvax 150 is basically a hot melt, having a melting point in the temperature range of 75°C to 80°C. Accepting that Elvax 150 is a block copolymer, as just described, then this melting point can be assigned to melting of the semicrystalline polyethylene block. Figure 13 is a plot of the melting point (T_m, °C) of polyethylene as a function of its average molecular weight as reproduced from Reference 21. Based on this plot, the average molecular weight of the polyethylene block in Elvax 150 can be estimated at about 2000 to 3000, which corresponds to a melting point in the range of 75°C to 80°C. With this information, and the compositional distribution of ethylene and vinyl acetate in Elvax 150, a molecular weight of about 2250 can be estimated for the amorphous, random-copolymer block.

These efforts to determine the chemical structure of Elvax 150, and perhaps of EVA resins in general, can provide a fundamental input for aiding interpretation of material properties, and changes in material properties that may result from outdoor exposure in a module application. In addition, structural information can be beneficial in guiding research directed toward identifying or developing potentially better antioxidant and UV stabilization systems. For example, the service longevity of Elvax 150 may be enhanced by use of a combination of antioxidants and other stabilization additives, each set of additives optimally selected for a specific block in the Elvax 150.

E. PRIMERS AND ADHESIVES

The first primer system developed (Reference 22) for EVA was for bonding the cured A-9918 EVA to glass. The composition of this primer is given in Table 10, and is referred to as the glass/EVA primer. Experimental quantities of this primer are available from Springborn Laboratories under the designation A-11861 Primer. As described in more detail below in this

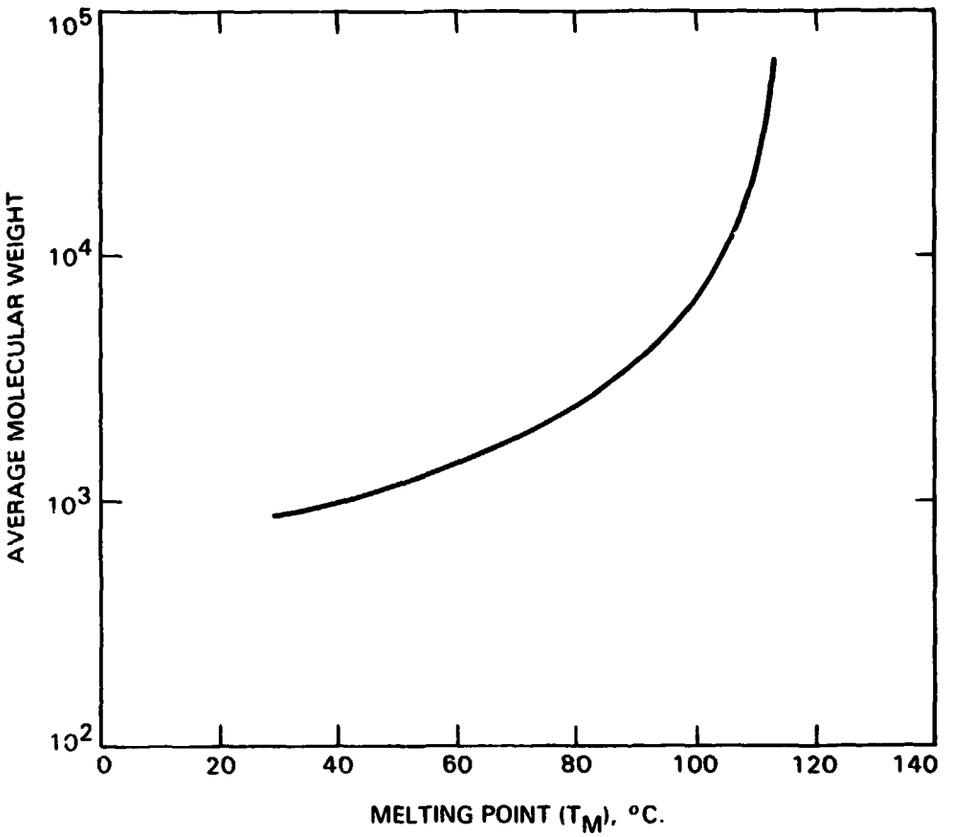

Figure 13. Melting Point vs Molecular Weight of Polyethylene

section, this glass/EVA primer resulted in very strong bonding to glass, under both dry and wet exposure conditions. This favorable experience with glass prompted a follow-on evaluation of this primer system for bonding EVA to many other materials. Immediate difficulties, however, were then encountered with copper, aluminum, Tedlar fluorocarbon films, and Scotchpar polyester films.

As copper and aluminum represent potential low-cost metals for solar-cell metallization, emphasis was next given to developing a primer system for bonding cured A-9918 EVA to these two metals. The composition of this metal/EVA primer is given in Table 10. Another primer system had to be developed separately for bonding cured A-9918 EVA to polyester films such as Scotchpar (3M Co.) and Mylar (Du Pont). The composition of this primer, referred to as the polyester/EVA primer, is given in Table 10.

For bonding cured A-9918 EVA to Tedlar film products, Du Pont identified an acrylic contact adhesive designated 68040. As supplied by Du Pont, the acrylic adhesive system is a solution in toluene, which is spread on the Tedlar surface and then allowed to dry. The resultant adhesive coating is dry and nontacky, and the coated Tedlar film can be wound and unwound. Experimental work with this adhesive system has used a coating thickness of 0.3 to 0.4 mil, which has yielded acceptable performance. The contact

Table 10. Glass, Metal, and Polyester Primers, and Tedlar Adhesive for A-9918 EVA

Component	Composition, parts by wt
Glass Primer (A-11861):	
Z-6030 silane (Dow Corning)	9.0
Benzyl dimethyl amine	1.0
Lupersol 101 (Pennwalt)	0.1
Methanol	90.0
Metal Primer:	
Z-6030 silane (Dow Corning)	99
Zinc chromate powder	100
Benzyl dimethyl amine	1
Methanol	300
Polyester Primer:	
Z-6040 silane (Dow Corning)	5
Resimene 740 (Monsanto)	95
Isopropanol	300
Tedlar Adhesive:	
68040 Acrylic contact adhesive (Du Pont)	

adhesive develops its bonding qualities at the high temperature of the EVA lamination cycle. A PV manufacturer may coat Tedlar optionally with the adhesive as part of its manufacturing operation, or arrange to have the coating put on by an independent coating vendor.

Table 11 is a master table of adhesive bond-strength measurements accumulated to date for cured EVA bonded to a variety of materials, with

Table 11. Adhesive Bond Strengths[a] for A-9918 EVA Bonded to Various Materials

Material	Primer	Bond Strengths, lb/in. of Width				
		Control	6 days Immersion		2 wk Immersion	2 h Boiling Water
			Without $ZnCrO_4$	With $ZnCrO_4$		
Sunadex Glass	A-11861	34.8	-		-	32.3
Window Glass	A-11861	39.6	-		37.9	27.1
Window Glass (Self-priming EVA)	A-11861	35.4	-		41.9	C
Galvanized Steel	A-11861	2.5	-		-	-
Mild Steel	A-11861	56.0	-		42.6	50.7
Aluminum	A-11861	41.0	-		2.3	2.6
Tedlar 100BG30UT	A-11861	4.5	-		-	0
Korad 212	A-11861	1.1	-		-	-
Scotchpar 20CP-White	Polyester	35.7	-		31.3	21.3
Aluminum	Metal	-	15.0	note 1	-	-
Mild Steel	Metal	-	11.0	17.6	-	-
Chrome Steel	Metal	-	1.1	note 1	-	-
Stainless Steel	Metal	-	4.4	19.8	-	-
Titanium	Metal	-	13.2	note 1	-	-
Brass	Metal	-	10.8	note 1	-	-
Copper	Metal	-	2.2	note 1	-	-
	Adhesive					
Tedlar 100 BG30UT	68040	6.2	-		note 2	7.8
Tedlar 200 BS30WH	68040	note 1	-		note 1	note 1
Tedlar 200 PT	68040	8.25	-		11.1	10.8

[a]Notes: 1. Cohesive failure in A-9918 EVA
2. Tedlar film tore during cell test

various combinations of the primers and the 68040 adhesive. These data, generated at different experimental laboratories, result from a similar experimental pattern: measurement of control values at ambient conditions, followed by measurement (again at ambient conditions) of specimens that have been immersed in water maintained at room temperature, and of specimens immersed in boiling water. The singular exception is work carried out with the metal/EVA primer system. For this system, metal/EVA bonded test specimens were prepared both with and without the zinc chromate powder in the primer formulation. Bond-strength measurements for these test specimens were made after 6 days' immersion in water maintained at room temperature, and no control values were measured.

The glass/EVA primer (A-11861) can be used optionally as either a wipe-on primer or as a compounding additive to generate a self-priming-EVA. If used as a compounding additive, the methanol solvent is not used, and the three-component mixture is blended into the EVA at a concentration of 1.0 wt %. A concept used in the formulation of this primer is that the addition of a small amount of the Lupersol 101 peroxide causes a localized generation of active free radicals during the heating and curing of the A-9918 EVA, resulting in a substantially higher crosslinking at the polymer-substrate interface.

The glass/EVA primer was tested by priming clean soda-lime glass slides with a thin layer of the primer (wiped on with a moistened pad) and air drying for 15 min. The fully formulated EVA compound (A-9918) was then compression-molded and cured against the surface. The resulting specimen was tested for peel strength by ASTM D-903. The results (Table 11) were excellent, yielding an average peel strength of 39.6 lb/in. of width. Duplicate specimens placed in boiling water for 2 hours and evaluated by the same process yielded an average peel strength of 27 lb/in. of width, still excellent adhesion. A quantity of the primer formulation was prepared without the alcohol diluent and blended into the standard A-9918 EVA formulation at 1 wt % to test the self-priming effect. The resulting resin was then compression-molded and cured against a clean glass slide, as before, and tested for peel strength by the same method. The average strength was 35.4 lb/in. of width (Table 11). The bond strength of the self-priming EVA after room-temperature water immersion for 2 wks increased from the initial value of 35.4 to 41.9 lb/in. of width.

As shown in Table 11, the glass/EVA primer not only gives excellent and durable bonds to regular soda-lime (microscope slides) and low-iron (Sunadex) glass, but also is marginally effective with aluminum, and very effective with mild steel. Aluminum, primed with A-11861, gave an average dry-bond peel strength of 41.0 lb/in. of width and the adhesion to mild steel was even higher, with an average dry strength of 56.0 lb/in. of width. This is the highest bond strength found between EVA and any other material. The wet-bond strength is excellent to mild steel and poor to aluminum. Dry-bond strengths to Tedlar were very low, and virtually zero when wet. The A-11861 primer was essentially ineffective for copper and for Scotchpar polyester film, for both dry and wet exposure conditions. On the other hand, the polyester/EVA primer worked excellently, yielding a dry control value of 35.3 lb/in., dropping slightly to 31.3 lb/in. after 2 wks of room-temperature water immersion, and still retained a high value of 21.3 lb/in. after 2 hours of immersion in boiling water.

The metal/EVA primer with zinc chromate powder achieved outstanding bonding of cured A-9918 EVA to aluminum and copper (Table 11), with peel testing resulting in cohesive failure of the EVA, after 6 days of water immersion. Cohesive failure of the cured EVA also occurred for bonding to chrome steel, titanium, and brass. The metal/EVA primer is apparently not as effective with mild steel as is the glass/EVA primer, A-11861, but the bond strength values of ≈17.6 lb/in. is still acceptably high. With the exception of mild steel, the action of zinc chromate on achieving substantial increases in bond strength can be observed in the performance data given in Table 11.

The two Tedlar films listed in Table 11, Tedlar 100BG30UT and Tedlar 200PT, are clear and transparent UV-screening films. The former is 1 mil thick and the latter is 2 mils thick. The third Tedlar film listed in Table 11, Tedlar 200BS30WH, is a 2-mil-thick white-pigmented film. The bond strength data given in Table 11 reveal that the 68040 adhesive yielded comparable wet and dry performance for the two UV screening films, and yielded outstanding performance with the white-pigmented Tedlar film. Involvement of the white-pigment material in enchancing the bond strength can only be conjectured.

With all three Tedlar films, the adhesive 68040 retained wet-bond strength, as compared with the zero bond strength of the glass/EVA primer (A-11861). For the 1-mil thick Tedlar 100BG30UT, the bond strength after 2 wks of room-temperature water immersion had apparently increased to a level where peel testing resulted in tearing of the Tedlar film.

One of the low-cost structural panel materials being investigated for module application is mild steel (Table 2), specifically cold-rolled mild steel. However, the concern with this material in an outdoor application is corrosion. An approach to corrosion prevention is adhesively bonding white-pigmented plastic films to both surfaces of a mild-steel panel. A trial film/adhesive/primer system has evolved, which consists of the following layers of materials on mild steel:

Outer film	Scotchpar 20CP-White
Primer	polyester/EVA primer
Adhesive	cured A-9918 EVA
Primer	metal/EVA primer
Panel	mild steel

Panels of mild steel coated with this film/adhesive/primer system have survived more than 4,500 hours of continuous exposure to salt spray (ASTM B-117) without any evidence of corrosion. Unprotected mild steel, on the other hand, begins to corrode within hours after exposure to salt spray. This use of EVA as an adhesive offers another possible application area for this low-cost material in terrestrial photovoltaic modules.

F. ENCAPSULATION ENGINEERING

An engineering analysis of encapsulation systems (Reference 9) was done to assess the effect of pottant properties and thickness on solar-cell stresses induced by thermal expansion and panel-bending loads. One of the goals of this analysis is a generation of guidelines for minimum material usage for each of the construction elements.

The analyses for structural adequacy showed that the thermal expansion or wind deflection of photovoltaic modules can result in the development of mechanical stresses in the encapsulated solar cells sufficient to cause cell breakage. The thermal stresses are developed from differences in the thermal expansion properties of the load-carrying panel and the solar cells. However, the analysis also showed that solar-cell stresses generated by either thermal expansion differences or wind deflection can be reduced by increasing the thickness t of the pottant, or by using pottants with lower Young's modulus E. In other words, the analysis indicates that the load-carrying panel can be considered to be the generator of stress, and that the pottant acts to dampen the transmission of the stress to the cells.

Computer predictions of the specific values of t and E have been carried out to date only for the analysis of a 4-ft square module, predicting the stress distribution throughout a module when deflected by a 100-mi/h wind (50 lb/ft^2 loading pressure), and predicting the stress distribution throughout a module set up by thermal-expansion stresses when the module is heated or cooled through a temperature difference of 100°C. For both cases, a zero-stress state was assumed to exist throughout the module before deflection or thermal stressing.

Construction details of the module that was analyzed are:

(1) Module dimension: 1.2-m (4 x 4-ft) square.

(2) Solar cells: 10 x 10-cm square (4 x 4 in. x 0.015 in. thick).

(3) Spacing between solar cells: 1.3 mm (0.050 in.).

For the deflection analysis, the perimeter of the module is assumed to be constrained and restricted from being twisted or deflected out of planarity. Thus, as the module deflects under a uniform wind-pressure load, the edges always remain in the plane of the undeflected, initially flat module.

Structural analysis was done on three encapsulation systems: glass superstrate, wooden substrate and mild-steel substrate designs. The structural properties of the glass, wood, and mild steel were fixed input data. The pottant was treated as a variable, expressed in terms of its Young's modulus E, and thickness t. Output data consisted of the prediction of the maximum stress developed in the solar cells, calculated as a function of pottant modulus and pottant thickness between the cells and the structural panel. The structural analysis model is summarized in Figure 14 and the structural properties used as fixed input data are given in Table 12. For the silicon solar cells, the maximum allowable stress in bending is 8000 $lb/in.^2$, and the maximum allowable stress in tension (thermal expansion) is 5000 $lb/in.^2$ (References 8, 9, and 23).

Table 12. Structural Parameters Used in Encapsulation Engineering Computer Studies

Material	Modulus, lb/in.^{2}	Thermal Coefficient, in./in.°C	Allowable Stress, lb/in^2
Tempered Glass	10×10^6	9.2×10^{-6}	13,000
Wood	$0.8\text{-}1.2 \times 10^6$	7.2×10^{-6}	2500
Silicon	17×10^6	4.4×10^{-6}	5000-8000
Steel	30×10^6	10.8×10^{-6}	28,000

The computer-predicted results are shown in Figures 15 through 20. The computer-predicted data traces for a Young's modulus E of 1000 lb/in.^{2} essentially correspond to those of cured A-9918 EVA, which has a Young's modulus E of (nominally) 890 lb/in.^{2} at 25°C (Table 6).

For the thermal stress analyses (ΔT = 100°C) (Figures 15, 16, and 17), the computer predictions indicate that a minimum thickness of 2 mils of EVA is

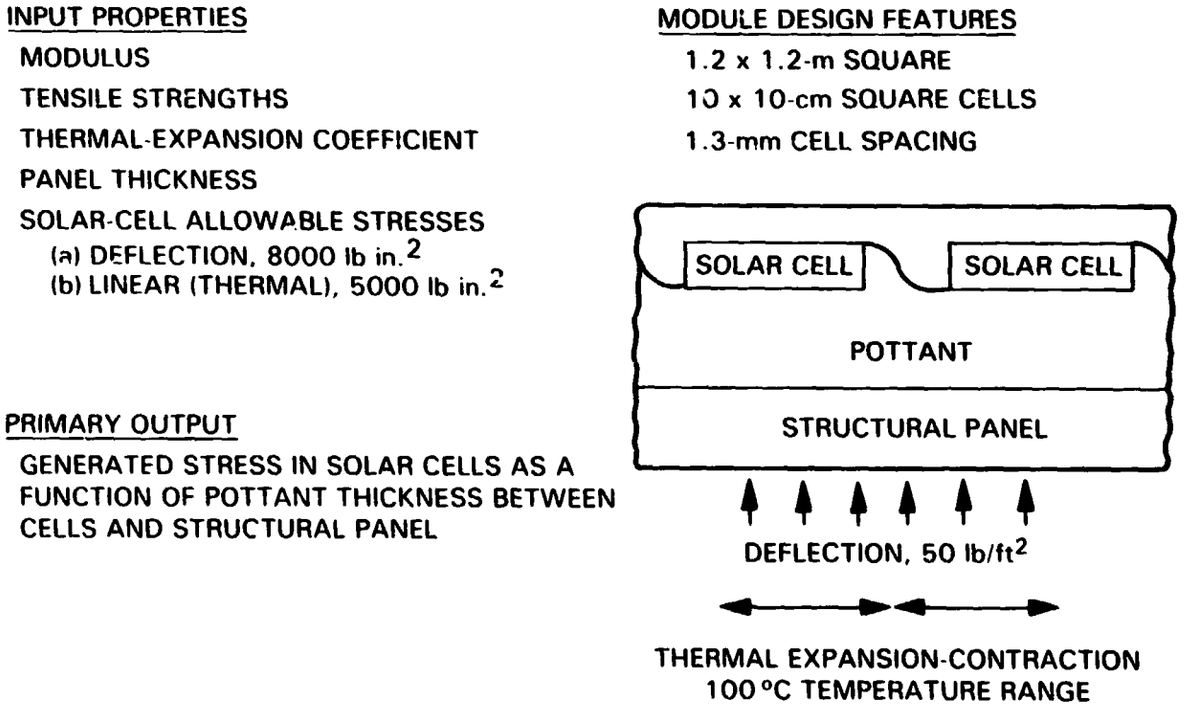

Figure 14. Structural Analysis: Deflection and Thermal Stress

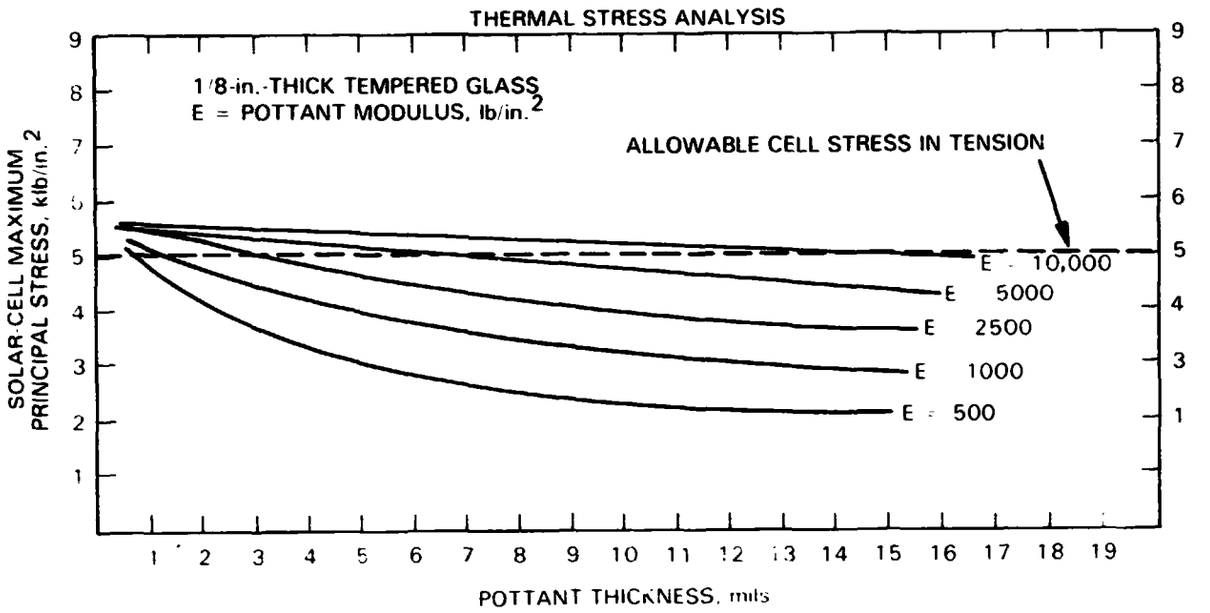

Figure 15. Computer-Predicted Stresses in Encapsulated Silicon Solar Cells Resulting From Thermal Expansion Differences in a Glass-Superstrate Module for ΔT of 100°C

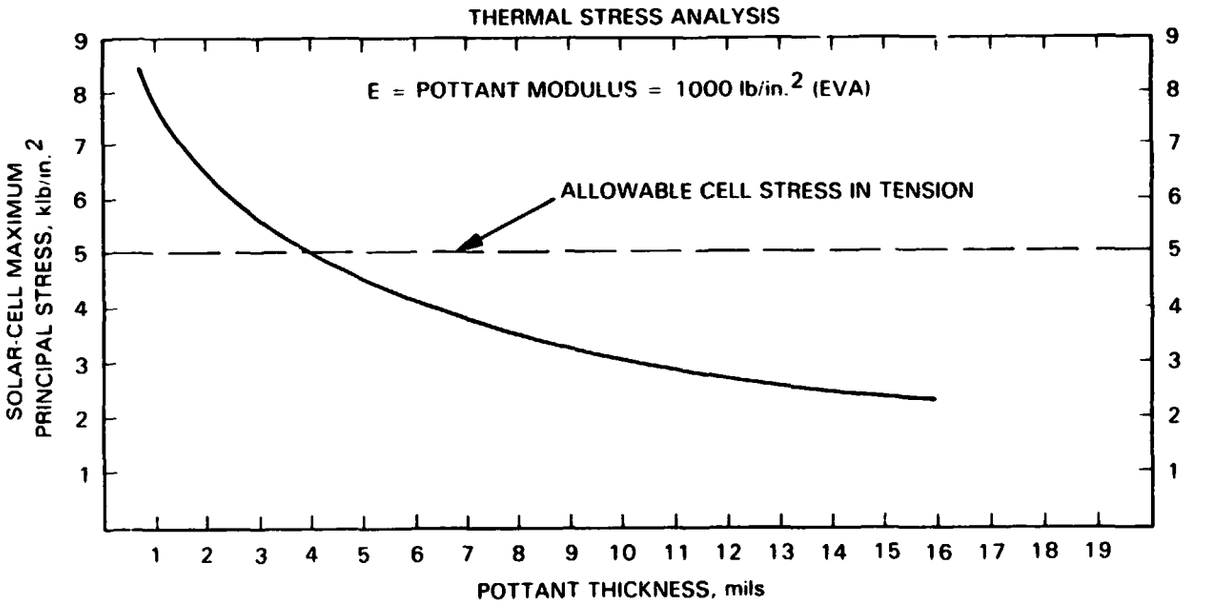

Figure 16. Computer-Predicted Stresses in Encapsulated Silicon Solar Cells Resulting From Thermal Expansion Differences in a Steel-Substrate Module for ΔT of 100°C

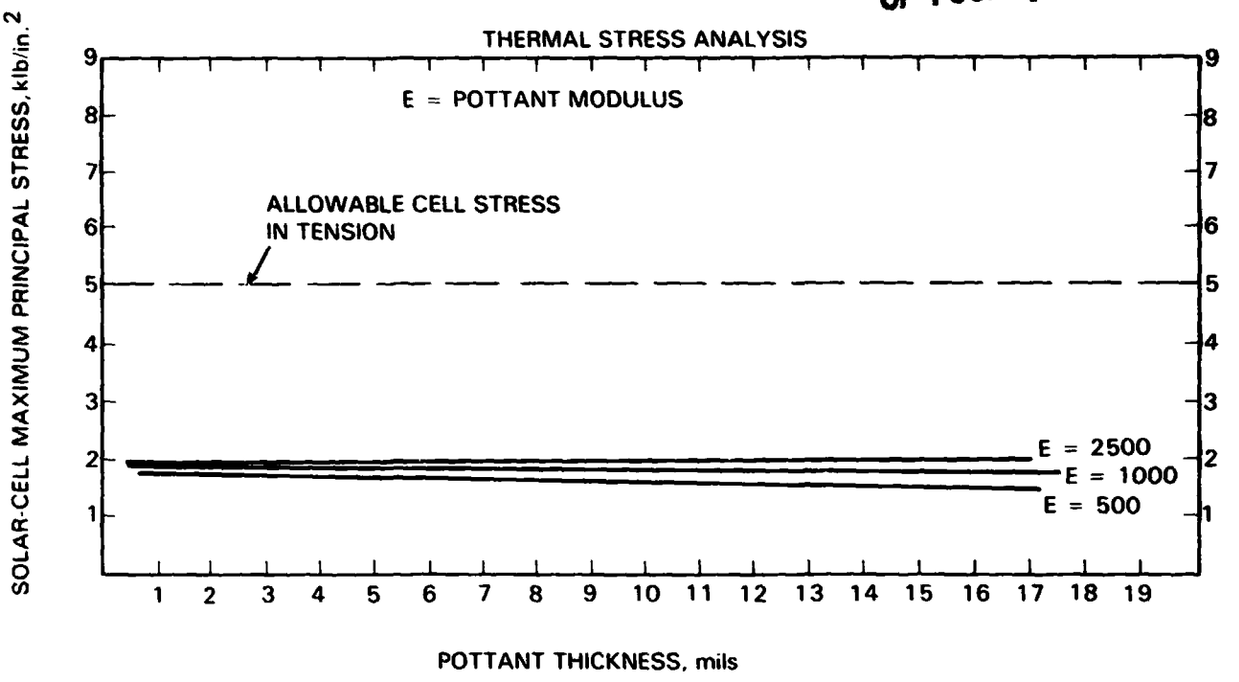

Figure 17. Computer-Predicted Stresses in Encapsulated Silicon Solar Cells Resulting From Thermal Expansion Differences in a Wooden-Substrate Module for ΔT of 100°C

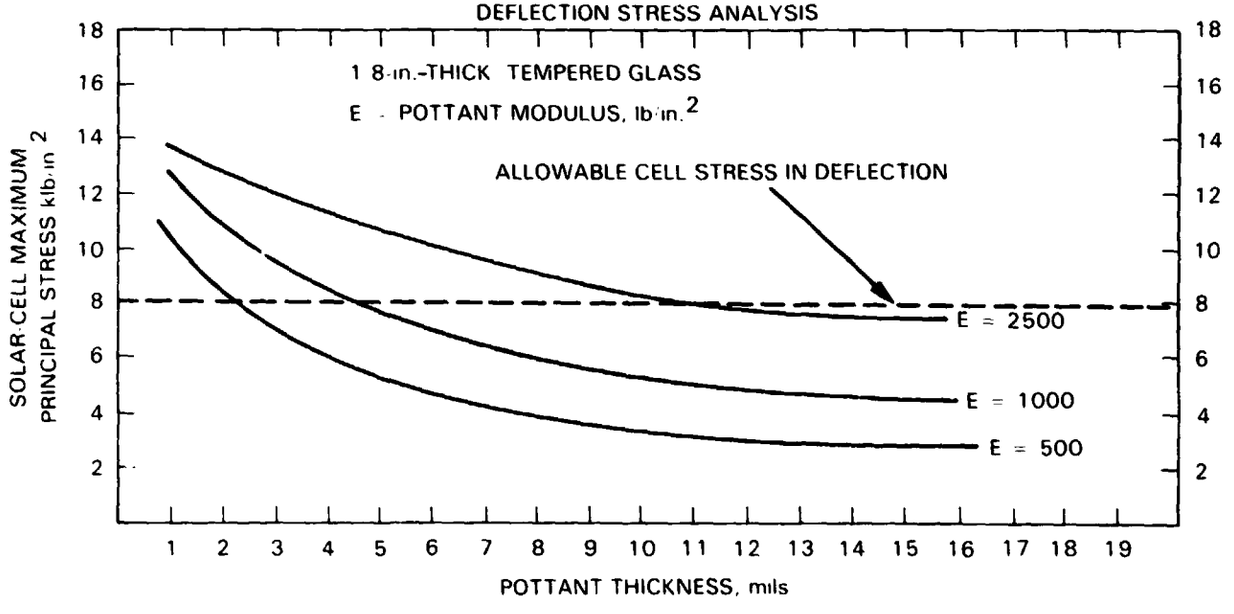

Figure 18. Computer-Predicted Stresses in Encapsulated Silicon Solar Cells Resulting From Deflection of a 4-ft-Square Glass-Substrate Module Under a Uniform Load of 50 lb/ft^2

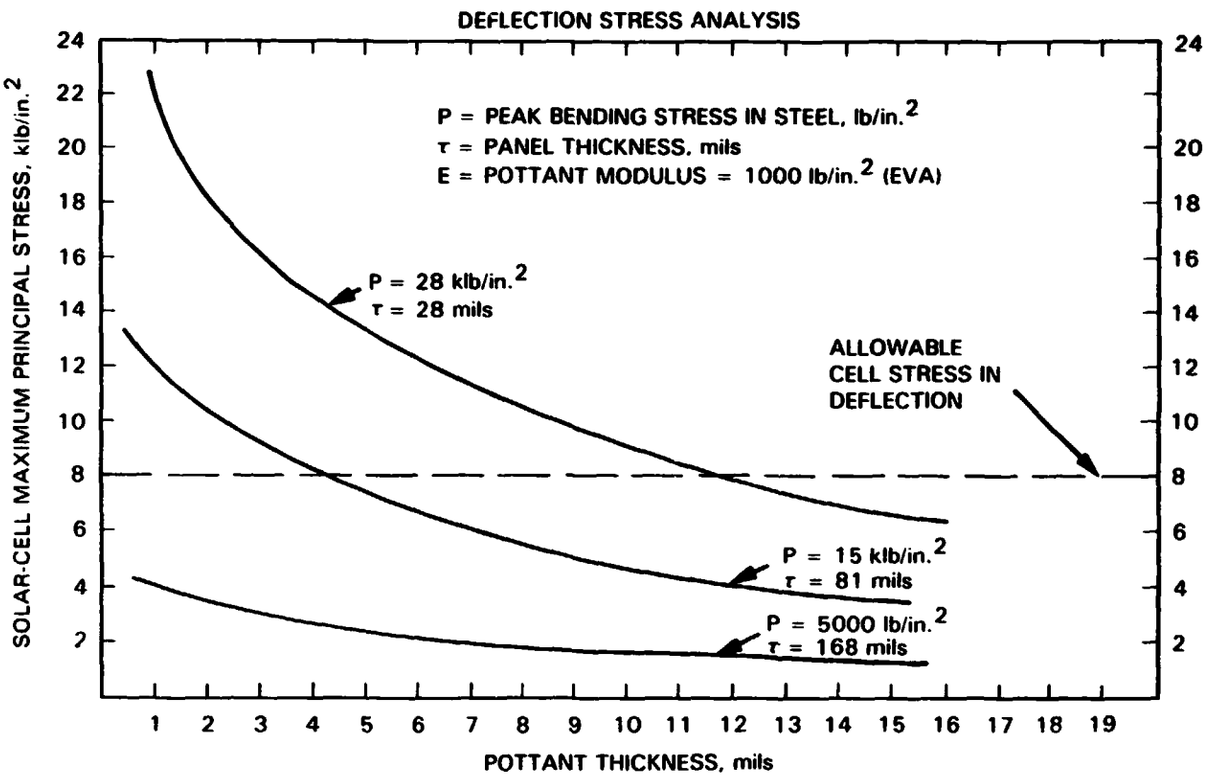

Figure 19. Computer-Predicted Stresses in Encapsulated Silicon Solar Cells Resulting from Deflection of 4-ft-Square Steel Panels of Three Different Thicknesses Under a Uniform Load of 50 lb/ft^2

required between the solar cells and a glass superstrate panel, and that a minimum thickness of 4 mils of EVA is required between the solar cells and a mild-steel substrate panel. These minimum thickness requirements are typically satisfied in a practical module, as the commercial thickness of EVA laminating film is 18 mils, which thins to about 10 mils in the module after lamination (References 5, 6, and 8). For the wooden-substrate panel (Figure 17) the closer match of their thermal expansion coefficients (Table 12) virtually eliminates any dependence on the EVA pottant thickness to reduce solar-cell stresses. Technology is being developed to virtually eliminate stresses due to expansion and contraction caused by humidity.

For wind deflection of a 1/8-in. thick glass superstrate module (Figure 18), a minimum thickness of 4 to 5 mils of EVA is required. This is thicker than needed for thermal stressing (Figure 15), and therefore deflection, rather than thermal stressing, controls the pottant-thickness requirements for a glass-superstrate module. Figure 19 plots the computer-predicted stresses in solar cells for mild-steel panels 28 mils, 87 mils, and 168 mils thick. As the steel panels become thicker, their stiffness against wind deflection increases, thus reducing the thickness requirements of the EVA pottant. Deflection analysis of a 1/8-in.-thick wooden-substrate module indicated that a wooden panel of this thickness would fracture under a wind loading of 50 lb/ft^2, but that a 1/4-in. wooden panel would not. However, for a 1/4-in.-thick wooden panel, a

minimum thickness of 13 mils of EVA is required, which exceeds the typical thickness of 10 mils ordinarily achieved in present-day modules when using an 18-mil laminating film. This deflection analysis indicates that a wooden substrate panel would have to be ribbed on its back side in order to increase its structural stiffness against wind deflection. The computer analysis of a ribbed, 1/8-in.-thick wooden panel design is shown in Figure 20, which indicates that this design approach results in sufficient panel stiffness to virtually eliminate any dependence on the EVA to reduce solar-cell stresses.

Further analysis of these computer results indicated that all of these data traces could be merged into reduced-variable master curves (Reference 24), which revealed that the pottant's ability to dampen solar-cell stresses is, in general, directly related to the ratio of its thickness to modulus, t/E. Using the data for the wind deflection of glass-superstrate modules as an illustration (Figure 18) the t/E ratio associated with the maximum allowable solar-cell stress of 8000 lb/in.^{2} is about 222; e.g.,

$$\frac{500}{2.25} = \frac{1000}{4.5} = \frac{2500}{11.25} = 222$$

This capability of expressing the structural engineering requirements of a pottant in a simple ratio of thickness to modulus enables a cost-comparison basis for candidate pottant materials. For example, compared to EVA, a higher-costing pottant with a higher Young's modulus would be much more costly to use, for reasons of both higher materials cost and the need for greater thickness. On the other hand, a higher-costing pottant having a lower Young's modulus may be just as cost effective because of an allowed reduced thickness.

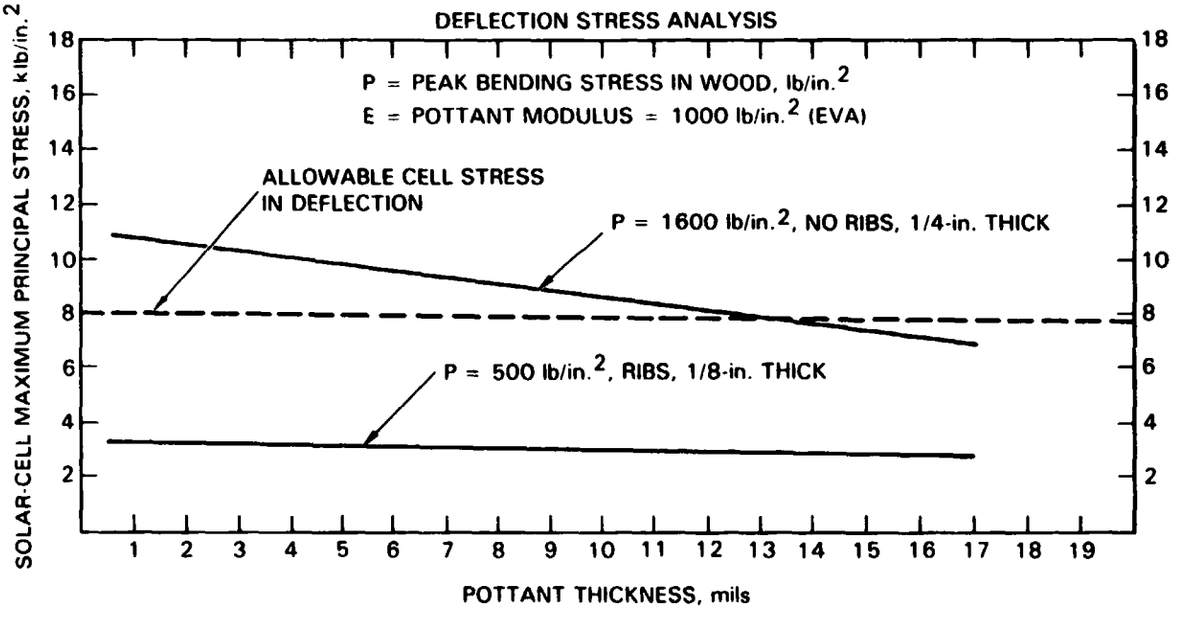

Figure 20. Computer-Predicted Stresses in Encapsulated Silicon Solar Cells Resulting from Deflection Under a Uniform Load of 50 lb/ft^2 of an Unribbed, 4-ft-Square, 1/4-in.-Thick Hardboard, and a Ribbed, 4-ft-Square, 1/8-in.-Thick Hardboard

G. EVA AGING STUDIES

This discussion is divided into four parts. The first part describes those functional properties of pottant materials identified to date as critical to module performance and life. The upper and lower bounds on these properties as currently perceived are described, and therefore an assessment of the allowable magnitude of the changes from initial values of these properties over the service life of a module can be appreciated. It is expected that additional critical properties may be identified from future aging studies or outdoor weathering experience.

The second part describes the known aging behavior of ethylene vinyl acetate resins at elevated temperatures, as reported in Du Pont technical literature for these products. The third part describes various experimental aging programs at different laboratories, and documents the aging results accumulated to date. It will be noticed that the properties being monitored for aging trends do not necessarily include all of the functional properties to be described in Part 1. This is because the various experimental aging programs were started, and were well under way, long before the need to monitor all of these specific properties was recognized.

The fourth part is a beginning effort at generating a unifying and fundamental hypothesis of the mechanisms of EVA aging.

With respect to the weather aging of a pottant in a PV module, the module design philosophy as described in Section II is to shield or isolate the pottant from exposure to those UV wavelengths that would activate UV photooxidation of the pottant. Alternatively, the pottant could be isolated from oxygen by being used in a hermetic module having, for example, a glass-superstrate cover and a metal-foil back cover. In essence, by eliminating exposure to harmful UV wavelengths and/or oxygen, the aging behavior of a pottant should be associated with purely thermal effects, such as thermal oxidation in a non-hermetic module, or possibly thermal decomposition in a hermetic module. UV protection (isolation) in a non-hermetic PV module is to be provided by use of a UV-filtering outer cover glass or plastic film, and by the use of UV absorbers (e.g., Cyasorb UV 531) compounded into the pottant. Thus some of the issues that must be considered in any study relating to the potential service life of a pottant are:

(1) Identification for a non-hermetic design of the deleterious UV wavelengths.
(2) Permanence of the UV protection schemes.
(3) Thermal aging behavior of the pottant, including the effects of antioxidants.

The UV absorption spectra of all of the components in A-9918 EVA, including the base material Elvax 150, are given in Figure 21. The peak UV absorption for Elvax 150 occurs at about 280 nm, and thereafter, with increasing wavelength, its UV absorption decreases, first rapidly in the range of 280 nm to about 310 nm, and then very gradually to become virtually zero (non-UV-absorbing) near 360 nm. Since only absorbed UV wavelengths can activate UV-related reactions, the absorption spectra indicate that the deleterious UV wavelengths for Elvax 150 would be those less than 360 nm. The protective UV-absorbing additive, Cyasorb UV 531, absorbs strongly in this

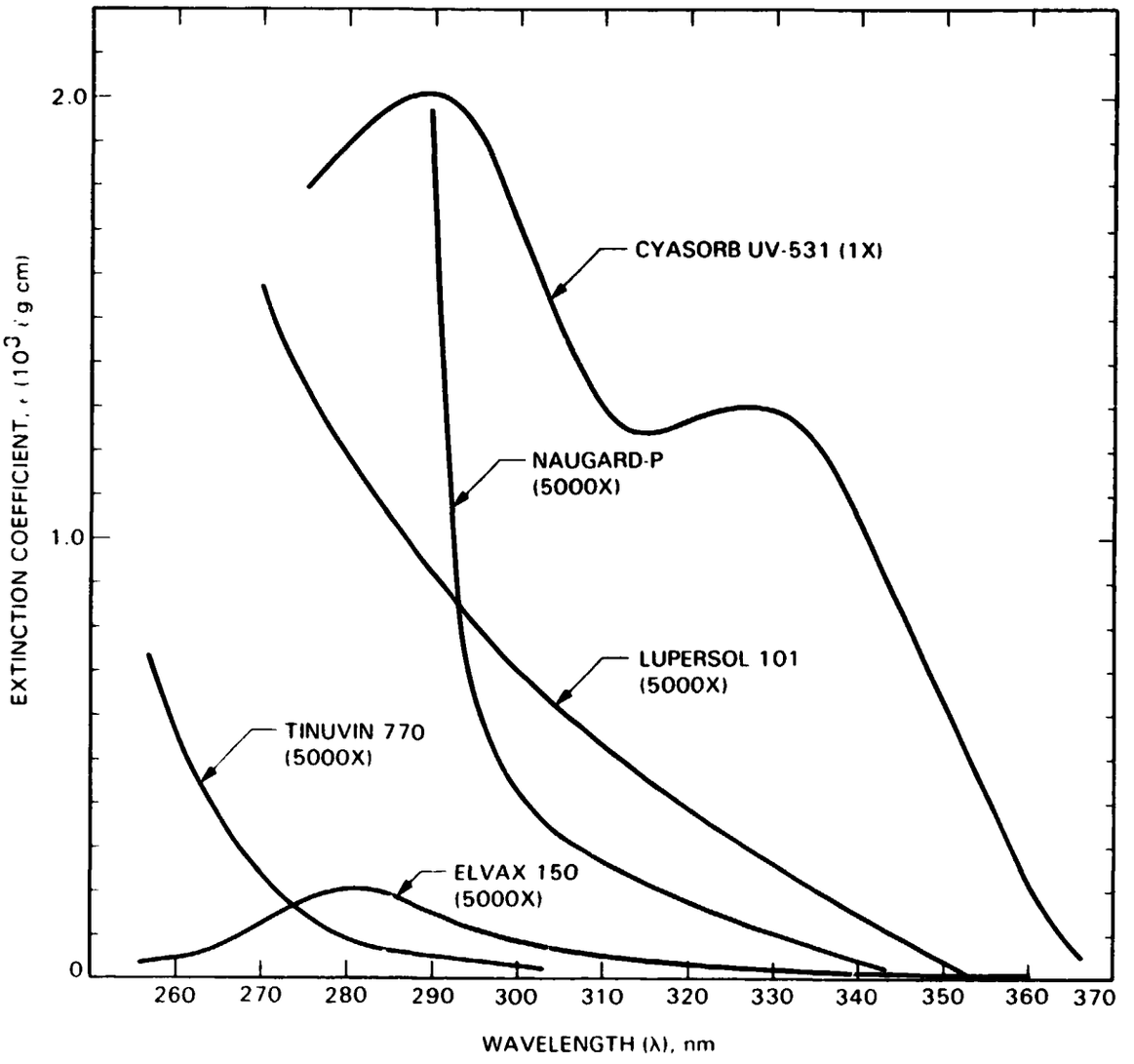

Figure 21. UV-Visible Absorption Spectra of Each Component in Formulated EVA A-9918

wavelength region, and therefore is expected to provide UV protection for the Elvax 150. However, since Cyasorb UV 531 is a compound of low molecular weight, a concern with this material is the potential for physical loss, and therefore loss of one element of the UV-protection scheme. Physical loss of Cyasorb UV-531 could occur, for example, by migration to module surfaces, where it could then be removed by rain or lost by evaporation. The other element of the UV-protection scheme involves UV-filtering glass or plastic film front covers. Glass will typically absorb UV wavelengths at and below 310 to 315 nm; therefore the requirement for a UV-absorbing additive such as Cyasorb UV-531 to protect EVA in the UV wavelength range between 315 nm and 360 nm becomes a necessity for a non-hermetic glass module. If Cyasorb UV-531 were to become depleted, glass alone without an oxygen barrier back cover may not be adequate to protect the EVA against UV photooxidation. The candidate UV-filtering plastic films, Acrylar and Tedlar, essentially absorb all UV

wavelengths below 360 nm (Reference 10), and therefore offer promise of providing total UV protection for the EVA. However, if these films were to lose their UV-absorbing property gradually during outdoor service, and since all plastic films are permeable to oxygen, then a UV-absorbing additive such as Cyasorb UV-531 provides backup protection against UV photooxidation.

Therefore, in terms of the permanence of the UV protection schemes, whether glass without an oxygen barrier back cover or plastic-film front cover, any loss of the UV-absorbing additive compounded into EVA could become critical. This consideration has prompted three basic studies:

(1) Analysis for Cyasorb UV-531 in EVA specimens being aged

(2) Investigation of aging effects on the UV-absorbing properties of the plastic films (Reference 10)

(3) Identification or development of UV-absorbing additives intrinsically resistant to physical loss (see Section III, H2).

1. Functional Properties

An FSA goal is to demonstrate a technical expectation of a potential 20-yr service life for terrestrial PV modules. When operating outdoors, peaking temperature levels from 55°C to 60°C can be expected for rack-mounted modules, and possibly up to 80°C to 85°C if a module is flush-mounted on an industrial or residential rooftop. As encapsulation pottants such as EVA are a component part of a module, then EVA if used must survive for 20 yr the continued and daily thermal cycling to these peaking temperature levels. That is, what must survive for 20 yr are those properties of EVA that are functionally required for module performance. Further, as it might be expected that these required functional properties may change through aging over 20 yr, their property value limits, both minimum and maximum, must be specified, which also aids in estimating allowable rates of change for comparison against actual rate of change observed in aging tests.

As of this writing, four functional properties required of a pottant such as EVA have been identified:

(1) Maximum optical transmission in the silicon solar-cell operating wavelength range of 0.4 to 1.1 μm.

(2) Necessary mechanical properties to maintain spatial containment of the solar cells and interconnects and to resist mechanical creep. The level of mechanical properties also must not exceed values that would impose undue mechanical stresses on the solar cell.

(3) Retention of a required level of electrical insulation to protect against electrical breakdown, arcing, etc., with the associated dangers of electrical fires, and hazards to human safety.

(4) Chemical inertness with encapsulated components such as the cells, metallization, interconnects, and electrical wiring.

Freshly cured and unaged A-9918 EVA has a total integrated light transmission of near 91.0% (Table 6). The value of 91.0% is not corrected for

surface reflection losses (Fresnel losses), which would be in the order of 8% for normal incident light. Ideally, aging should not result in a decrease in light transmission, which would then directly result in a decreased power output from the solar cells. Currently, it is a goal that the module power output shall not decrease after 20 yr to less than 75% of the initial value. Power decrease from a module can occur from light obscuration associated with surface soiling, a decline in efficiency of performance of the cells themselves resulting from corrosion effects, interconnect failures, and other circuit problems, and/or from a decrease in light transmission of the pottant (e.g., EVA) caused by aging. If, of the initial 100% of module power output, 5% of loss is allocated to soiling (References 25, 26, 27), 10% of loss to cells and circuit problems, then the remaining 10% of allowed loss can be tentatively allocated to loss of light transmission of the pottant. For EVA, this would roughly amount to a decrease from an initial measured value of 91.0%, to no less than 82%. It is not expected that weather-caused aging would result in an increase in optical transmission.

Two mechanical properties have been identified as critical: creep and Young's modulus. With respect to creep, EVA must be cured (crosslinked) in order to develop resistance against melt, flow, and creep at service temperatures higher than 70°C. Trial-and-error experimentation showed that EVA must be cured to a minimum gel content of 65% in order to develop creep resistance at 90°C. The temperature of 90°C was adopted on the basis of a module qualification test developed at JPL, which thermally cycled vertically aligned modules between -40°C and +90°C (Reference 28). For gel content less than 65%, the EVA in a vertically aligned module would creep and flow at the upper temperature of the thermal-cycle test. Gel content of properly cured A-9918 EVA will typically be in excess of 75%, with attendent creep resistance at 90°C. Aging of cured A-9918 EVA should not result in a reduction in gel content below 65%, over the expected service lifetime of 20 yr, especially for sloped-rooftop applications where peak service temperatures in the order of 80°C to 85°C can be expected.

With respect to Young's modulus, encapsulation engineering analysis (see Section III, F) has indicated that the level of mechanical stresses developed in encapsulated solar cells, arising from wind-caused module deflections or thermal expansion mismatches, can be decreased either by increasing the thickness of pottant between the cells and the structural panel, or by reducing the Young's modulus of the pottant. The analytical modeling enabled the development of connective relationships between the thickness t of the pottants, its tensile modulus E, and the maximum allowable stress levels in solar cells, in order to reduce the risk of solar cell breakage. The attenuating factor for pottants is related to the ratio of thickness to modulus, t/E, and as noted above, increasing t or decreasing E acts to reduce solar-cell stresses. A consequence of this analytical modeling is the indication that for most practical module designs having a pottant thickness of about 10 mils, the tensile modulus of the pottant as measured at 25°C probably should not exceed 3000 lb/in.^{2}. The tensile modulus of properly cured, unaged A-9918 EVA is in the order of 890 lb/in.^{2} (Table 6).

Analytical modeling is helping to provide an upper bound to Young's modulus, but an absolute lower bound has not yet been determined. Nevertheless, if aging were to lower the Young's modulus of A-9918 EVA, that would be the mechanically favored direction.

For chemical inertness, quantifiable techniques and measurement methods have not yet been worked out, nor has an organized and specifically directed aging program to evaluate chemical inertness been initiated. However, some early and very preliminary trial testing (Reference 15) was carried out at 130° with clean, shiny copper discs encapsulated in cured A-9918 EVA. At this aging temperature, strong yellowing discoloration of the EVA and tarnishing of the copper discs was visible within 90 hours. For these tests, the metal/EVA primer (Table 10) developed for bonding EVA to copper was not used. A major aging program on chemical inertness is being planned.

For electrical insulation, current FSA requirements call out the following for a pottant material (Reference 29):

(1) Minimum thickness to withstand breakdown from a dc voltage difference of 3000 V across the thickness. The average dielectric strength of EVA is about 600 V/mil (Table 6). and therefore a minimum 5 mils of thickness is needed. In practice however, the typical thickness of EVA in a module exceeds 10 mils. If this manufacturing practice were to continue, and aging were to reduce the dielectric strength of EVA a lower-bound value in the order of 250 V/mil becomes apparent.

(2) Leakage current across the thickness direction of the pottant at 1500 volts dc shall be less than 50 μA. The leakage current at 1500 volts dc across a 10-mil-thick sheet of cured, unaged A-9918 EVA is less than 0.2 μA. Therefore, the upper-bound allowable from the weather aging of A-9918 EVA is 50 μA, per the present requirement callout.

2. Known Aging Behavior of EVA

Du Pont Technical Bulletin 0820.2 reports that the purely thermal degradation of ethyl vinyl acetate resins, in the absent of oxygen and water vapor, proceeds by the conversion of acetate groups to acetic acid, followed by crosslinking at the resultant sites of unsaturation, and ultimately gelation. The thermal degradation rate versus temperature for the conversion of acetate groups to acetic acid is shown in Figure 22, which is reproduced from Technical Bulletin 0820.2. Note that significant conversion only occurs at very high temperatures, which can occur during certain high-temperature processing operations, but that at temperatures close to roof-top temperatures, 200°F (93.3°C), the conversion rate is an almost negligibly low value of 6.3×10^{-10}% per minute ($\log k = -9.2$). If the EVA were sustained continuously at 200°F (93.3°C) for 20 yr in the absence of oxygen and water vapor, this would correspond to a net conversion of only 0.006% of the acetate groups to acetic acid. On an absolute weight basis, this would correspond after 20 yr to an acetic acid accumulation of less than 0.002 wt % in the A-9918 EVA pottant. A hermetic module design comprising a glass superstrate and a metal-foil back cover essentially would isolate the EVA pottant from exposure to atmospheric oxygen and water vapor, and with only a few hours per day at which the module would be at rooftop peaking temperatures, a problem associated with acetic acid generation over 20 yr appears remote. No problem is expected with a hermetic module design at array peaking temperatures of 55°C to 60°C.

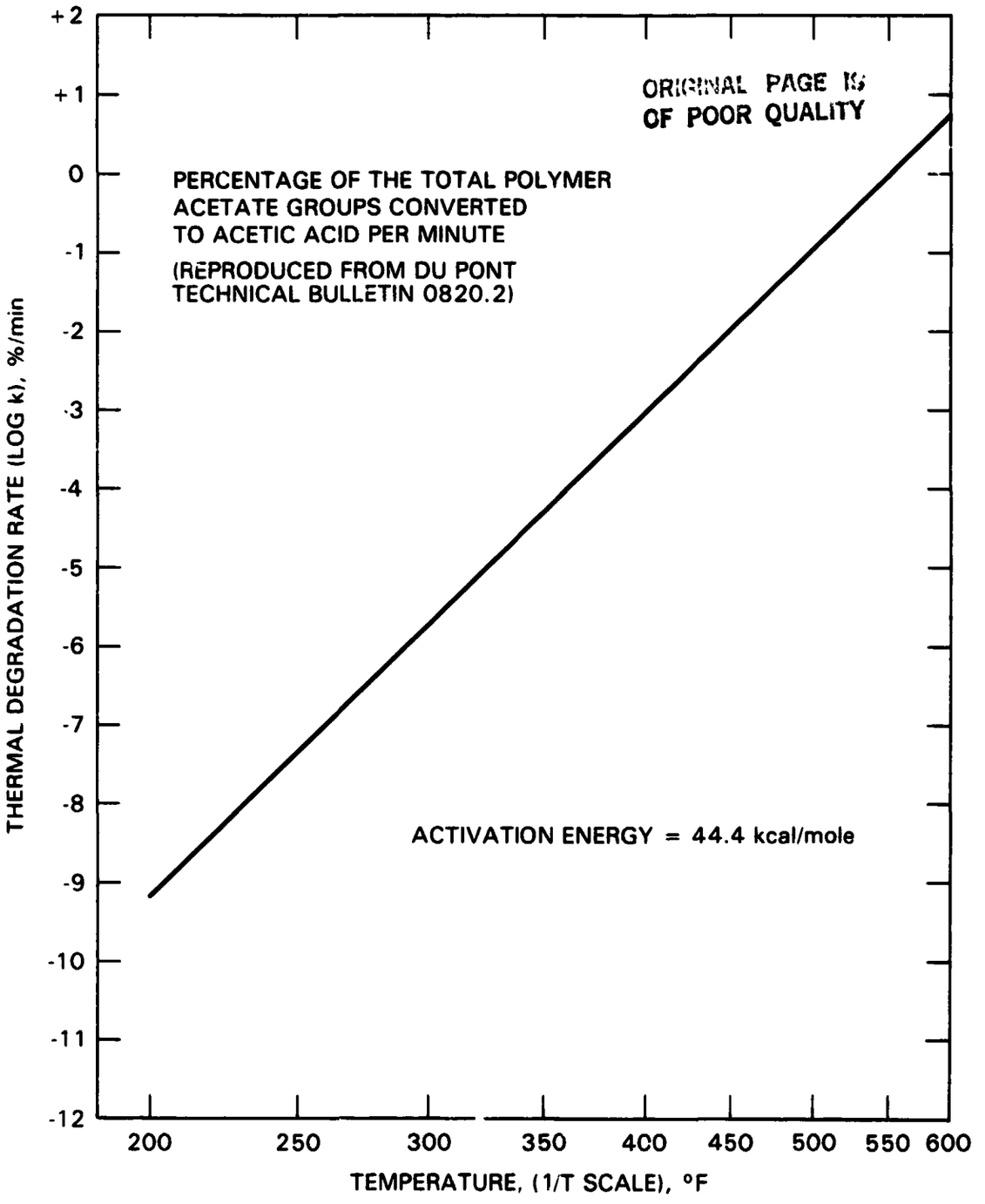

Figure 22. Thermal Degradation of Elvax Vinyl Resins

In a substrate design with a plastic film front cover however, exposure of the EVA pottant to atmospheric oxygen and water vapor can occur, as all plastic films are permeable by these gases (Reference 14). A search of public literature has not as yet uncovered any reports or articles on the effects, if any, of atmospheric oxygen and/or water vapor on acetic acid generation.

Therefore, chemical analysis for acetic acid is included as part of the EVA experimental aging studies. The concern with acetic acid generation, if it should occur in any quantity, is twofold: first, the potential for chemical corrosion of any metals encapsulated within the EVA (chemical inertness), and second, the potential for loss of the EVA's electrical insulation effectiveness, through an increase in leakage current and/or a decrease in dielectric strength.

3. Experimental EVA Aging Programs

The aging behavior of both Elvax 150 and the cured A-9918 EVA are being studied at Springborn Laboratories and at JPL. A summary of their separate aging programs and essential findings to date are given respectively in Tables 13 and 14. Details of each of these programs will first be separately described, and then their results will be combined to generate an evolving picture of the aging behavior of this material and an assessment of the materials' service-life potential for array and rooftop-module applications.

a. Springborn Laboratories. Springborn has carried out thermal aging (in the dark) of cured A-9918 EVA at 70°C, 90°C, and 130°C in air-circulated ovens, and has exposed Elvax 150 and cured A-9918 EVA to UV light at 55°C. The UV light source is a General Electric RS/4 sunlamp, which is filtered to remove nonterrestrial wavelengths below 295 to 300 nm. The UV spectra and intensity from these lamps at the sample location have been measured (Reference 30), and when compared with the peak intensities of AM1.5 natural sunlight, correspond to an average UV intensity of about 1.4 suns. If it is assumed that typical values of total annual UV insolation in the United States (Reference 31) were delivered at AM1.5 peak intensities, this would correspond to about 5 hours per 24-hour day to deliver the total annual UV insolation. Thus, defining a 1-sun UV day as 5 hours in each 24-hour day, then about 1300 hours of exposure to these RS/4 sunlamps operating at 1.4 suns UV intensity represent one year of outdoor UV exposure. The UV exposure temperature of 55°C was selected to match array peaking temperatures. Atmospheric moisture in the RS/4 test chambers and in the air-circulated ovens is that associated with the laboratory environment, typically at a relative humidity of about 50% to 60% at 25°C (77°F).

Exposure of unprotected Elvax 150 to RS/4 UV at 55°C results within 1000 hours in a visible onset of yellowing, which continues and becomes more intense with continued exposure. The surface of this material becomes stick and tacky, and the physical shape of the specimen eventually manifests slump and a tendency to flow. Progressive deterioration led to termination of this aging test at 1500 hours. Exposure of an Elvax 150 sample crosslinked with 1.5 pph of Lupersol 101, but which contained none of the stabilization additives listed in Table 3, essentially paralleled the aging behavior of the uncrosslinked Elvax 150. The primary difference was general retention of its initial physical form, presumably a result of the effect of crosslinking. Progressive deterioration involving yellowing and surface stickiness resulted in termination of this aging test also at 1500 hours. Crosslinking of Elvax 150 alone was insufficient to stop or suppress the action of UV photooxidation.

Table 13. Summary of EVA Aging Program at Springborn Laboratories

Aging Conditions	Test Specimens and Experimental Status
UV Aging Temperature, 55°C; UV source, RS/4 sunlamps (GE); Ambient relative humidity	Elvax 150: terminated after 1500 h; light-yellow color, sticky surface Elvax 150 cured with Lupersol 101: terminated after 1500 h, light-yellow color, sticky surface Elvax 150 behind a UV-screening film: system failure forced termination at ≈22,000 h. At routine inspection after 21,231 h, Elvax 150 was visually in excellent condition, with no visible color, and a firm and non-tacky surface Cured A-9918 EVA: has accumulated nearly 30,000 h of exposure to April, 1982, and is continuing; no visible change; time trend of measured properties given in Table 15
Dark Thermal Aging Aging in air-circulated ovens at 70°C, 90°C and 130°C; Ambient relative humidity	Cured A-9918 EVA specimens only: specimens have accumulated 10 mo (7200 h) of thermal aging to April 1982, and continuing; no visible change in specimens aged at 70°C and 90°C; definite yellowing and deterioration of specimens aged at 130°C; time trend of measured properties given in Table 16.

A specimen of uncrosslinked and uncompounded Elvax 150, positioned behind a UV-screening acrylic film, survived more than 21,000 hours of RS/4 exposure at 55°C without any visible evidence of yellowing or physical slump, and without any development of surface stickiness or tack. The acrylic film cover filters out all UV wavelengths shorter than 360 to 365 nm. Unfortunately, within a few hours after the routine visual inspection of this sample at 21,231 hours, the temperature regulator controlling the test temperature at 55°C failed, and the sample was heated to destruction, precluding the planned measurement of mechanical properties of the aged specimen. This test, nevertheless, strongly suggested that the UV wavelengths necessary for activating UV photooxidation were filtered out by the UV screen, and that without these wavelengths incident on the Elvax 150, this material was merely experiencing the equivalent of dark thermal aging at 55°C. The evidence therefore further suggests that to the time limit of this exposure, Elvax 150 exhibits natural resistance to thermal oxidation at 55°C.

Table 14. Summary of EVA Aging Program at Jet Propulsion Laboratory

Aging Conditions	Test Specimens and Experimental Status
UV Aging (6 suns intensity) Temperatures: 30°C, 70°C, 85°C, 105°C UV Source: Medium-pressure mercury lamp Ambient relative humidity	At Test Temperature 30°C: Elvax 150: terminated after 600 h; developed yellow color, sticky surface, partial crosslinking to generate insoluble gel phase Cured A-9918 EVA: terminated after 1400 h; only detected changes were harmless depletion of residual peroxide curing agent and trace generation of hydroxyl groups; no other changes At Test Temperatures 70°C, 85°C, 105°C: Cured A-9918 EVA: terminated after 400 h at 70°C and 800 h at 85°C and 105°C; in general, for specimens aged at 70°C and 85°C, changes were same as detected at 30°C, otherwise specimens were in excellent condition, including no visible yellowing; at 105°C, however, major property changes occurred, and the samples yellowed visibly (see text for details) Cured A-9918 EVA sealed between UV filtering Pyrex glass covers (with open edges): terminated after 400 h at 70°C, and 800 h at 85°C and 105°C; no visible yellowing in any specimens was detected, and a trace of acetic acid was detected only in the sample aged at 105°C
Dark Thermal Aging Temperatures: 30°C, 70°C, 85°C, 105°C Ambient relative humidity	At Test Temperature 30°C: Elvax 150: terminated after 500 h, no change Cured A-9918 EVA: Terminated after 1400 h, no change At Test Temperatures 70°C, 85°C, 105°C: Cured A-9918 EVA specimens only: terminated after 400 h at 70°C, and 800 h at 85°C and 105°C; no changes at 70°C and 85°C, visible yellowing of sample aged at 105°C

Specimens of cured and fully compounded A-9918 EVA were also directly exposed to RS/4 UV at 55°C. No UV-screening films or covers were used. This exposure test involved two different lots of cured A-9918 EVA. As a trial experiment, a small piece of cured A-9918 EVA was exposed to RS/4 to assess visually the aging behavior of this material. When this sample passed 3000 hours of exposure without any visual changes, it was decided to initiate exposure of a larger quantity of cured A-9918 specimens in order to monitor optical and mechanical properties as a function of aging time. The initial specimen, designated Lot 1, was left in the RS/4 chamber to continue accumulating exposure time, and the new batch of cured A-9918 EVA specimens were designated as Lot 2.

The optical and mechanical properties of Lot 2 A-9918 EVA, with up to 27,000 hours of UV exposure at 55°C, are given in Table 15. Up to 27,000 hours there was very little change in the measured properties of the cured A-9918 EVA. The sample removed for testing at 27,000 hours was clear, had no visible indications of any yellowing, was firm and non-sticky to the touch, and exhibited no slump or change in its physical form. The Lot 1 sample, having then accumulated 30,000 hours of exposure time, was also clear, with no indications of yellowing; it was firm, non-sticky, and without change in its physical form.

Accepting that 1300 hours of RS/4 exposure at 55°C equates to 1 yr of outdoor exposure at 55°C, then 27,000 to 30,000 hours would correspond to more than 20 yr of outdoor UV exposure. For an array installation having a peaking temperature near 55°C, these RS/4 data trends strongly indicate the potential of 20-yr service life for cured A-9918 EVA, used either in a superstrate or substrate module design. Further, as indicated above, Elvax 150 itself appears to be resistant against purely thermal aging at 55°C, but will yellow and age at 55°C when directly exposed to UV. Therefore, the deleterious UV wavelengths activating yellowing and aging by UV photooxidation are apparently filtered out by the UV screening film, and also by the Cyasorb UV-531 in the compounded A-9918 EVA. These aging tests at 55°C strongly indicated that the service longevity of EVA in a module operating at array peaking temperatures of near 55°C is not related to thermal oxidation concerns, but to the performance of the UV protection schemes.

Thermal aging in dark, air-circulated ovens of a third lot of cured A-9918 EVA was carried out for 10 mo at 70°C, 90°C, and 130°C. The test results for these thermally aged A-9918 EVA specimens are given in Table 16. Experimentally, the specimens aged 1 wk, 3 wks, and 2 mo were visually examined, and only their mechanical properties, consisting of tensile strength and of elongation at break, were measured. The test specimen aged for 10 mo at 70°C was lost. For the test specimens aged 10 mo at 90°C and 130°C, additional measurements of gel content, optical transmission, and Young's modulus were made.

After 10 mo of thermal aging at 90°C, there was essentially no change in the A-9918 EVA. This same behavior was observed for the 2 mo of thermal aging at 70°C. At 130°C, however, the A-9918 EVA underwent considerable deterioration from thermal oxidation. The material turned brown/orange in color, and experienced significant deterioration of both optical and mechanical properties. A trace of visible yellowing was noted after 1 wk of thermal aging at 130°C, and was very intense after 2 mo. Without even

Table 15. Properties of Cured A-9918 EVA as a Function of Exposure Time to RS/4 UV at 55°C

Lot 2 Specimens	Total Integrated Limit Transmission[a], %	Tensile Strength at Break, lb/in^2	Elongation at Break, %
Control	91.0	1890	510
2,880 h	91.0	1930	631
5,760 h	90.5	1340	550
8,640 h	90.0	1460	590
15,120 h	90.0	1520	570
27,000 h	90.0	1870	560

[a]Measured over the wavelength range 350 nm to 800 nm

considering UV, non-hermetic photovoltaic modules such as substrate designs, which will allow exposure of the A-9918 EVA encapsulant to atmospheric oxygen, and operating at 130°C, will probably experience eventual thermal oxidative yellowing and deterioration of the A-9918 EVA.

Ordinarily however, such high temperatures in photovoltaic modules are localized, associated with the overheating of a failed solar cell, which is referred to as solar-cell hot-spotting. The peak temperatures associated with solar-cell hot-spotting can be reduced by the use of bypass diodes in the electrical circuitry, and at the present time, these thermal aging results suggest for A-9918 EVA that the allowable peak temperature of a hot solar cell in a non-hermetic module design probably resides somewhere between 90°C and 130°C. Although the overall thermal aging behavior at 130°C of cured A-9918 EVA in a hermetic environment (that is, isolation from atmospheric oxygen and water vapor) has not yet been studied, the known potential for acetic acid generation suggests that the peak temperature of hot solar cells in a hermetic module design should also be limited to less than 130°C.

With respect to rooftop applications, and with the module design philosophy of shielding the A-9918 EVA from harmful UV, the thermal aging behavior at 90°C is initially very encouraging if it is assumed that the temperature of a rooftop-mounted module is at its peak temperature for about 5 hours each day; therefore the 10 mo (7200 hours) of thermal aging at 90°C corresponds roughly to almost 4 yr of rooftop service. Although encouraging, it is not known at this time whether the 10 mo of thermal oxidative stability at 90°C is a natural property of the Elvax 150, or a result of oxidative

Table 16. Thermal Aging of Cured A-9918 EVA in Circulating-Air Ovens

Time	Property	70°C	90°C	130°C
1 wk (168 h)	Tensile, lb/in.^{2}	2685	2200	2000
	Ult. elongation, %	595	550	550
3 wks (504 h)	Tensile, lb/in.^{2}	1700	1800	1240
	Ult. elongation, %	670	680	638
2 mo (1344 h)	Tensile, lb/in.^{2}	2370	2660	1320
	Ult. elongation, %	600	784	647
10 mo (7200 h)	Tensile, lb/in.^{2}	specimen	2120	144
	Ult. elongation, %	lost	660	37
	Gel content, %		91%	88%
	Color		clear, no yellow	brown/ orange
	Optical transmission, %		91%	74%
	Tangent modulus, lb/in.^{2}		833	335
Control (Unaged)				
	Tensile, lb/in.^{2}	2160		
	Ult. elongation, %	677		
	Tangent modulus, lb/in.^{2}	890		
	Optical transmission, %	91		
	Gel content, %	91		

protection afforded by the Naugard-P antioxidant. If the latter, oxidative protection will cease once the antioxidant has been sacrifically depleted. Detailed studies in this area are being initiated.

b. JPL. JPL has carried out UV aging and thermal aging (in the dark) of both Elvax 150 and cured A-9918 EVA. The dark and UV aging of Elvax 150 was carried out at 30°C only, whereas the dark and UV aging of cured A-9918 EVA were carried out at 30°C, 70°C, 85°C, and 105°C. For UV aging at 70°C, 85°C, and 105°C (but not at 30°C), additional test specimens consisting of cured A-9918 EVA positioned between UV-filtering Pyrex glass covers were also tested. These specimens were intended to simulate a hermetic module

design, although the narrow edges of these glass-sandwich specimens were unsealed. The UV light source was a medium-pressure mercury lamp, which generated an output of about 6 suns of UV intensity at the sample locations (Reference 10). These lamps were filtered to remove non terrestrial UV wavelengths. Assuming a 1-sun UV day as 5 hours for each 24 hours, then about 300 hours of exposure to this UV source equates with 1 yr of outdoor UV exposure. A summary of the JPL EVA-aging program is given in Table 14.

The test methods and techniques employed at JPL to monitor material changes due to aging were intended to provide information of a fundamental chemical nature; therefore, in general, engineering properties were not measured. For example, the UV-visible-IR absorption spectra of almost all of the test specimens were monitored primarily to detect changes in absorption spectra for chemical information, rather than to determine optical transmission relative to solar-cell performance. Particular emphasis was given to the sensitive detection of absorbance at 360 nm and 400 nm. Absorbance at 360 nm was used to monitor the concentration of Cyasorb UV-531 in the specimens, and absorbance at 400 nm was used to have a more sensitive monitor of material yellowing that may not be readily visible to the human eye.

Such monitoring at 400 nm resulted in the detection of what tentatively appears to be two distinctly different yellowing properties. The first is a transient yellowing, generally at low levels of intensity not detectable by the human eye, which is associated with the decomposition of the residual Lupersol 101 peroxide curing agent not consumed during the EVA cure. The second yellowing behavior is associated with thermal and/or UV photooxidation, which can eventually become visible to the human eye, as was observed in the Springborn aging test.

The kinetics of the thermal decomposition of Lupersol 101 peroxide is first-order, and an Arrhenius plot of the temperature dependence of the first-order reaction rate constant is shown in Figure 23. Evidence from the JPL test results indicate that for those A-9918 EVA specimens aged in the dark, and for those specimens exposed to UV but sandwiched between the Pyrex glass covers, the decomposition of the residual Lupersol 101 proceeds thermally in conformance with the rates given in Figure 23. But for those specimens directly exposed to the UV light, the decomposition rate of the residual peroxide is greatly accelerated. The time period of the transient yellowing is associated with the time period of active Lupersol 101 decomposition, whether it be thermal or accelerated by direct UV exposure. Indications from the JPL test results suggest that the decomposition of the residual peroxide proceeds harmlessly.

In general, the EVA aging trends observed at Springborn and at JPL were similar. At JPL, exposure of Elvax 150 to 6 suns of UV at 30°C resulted in visible deterioration within 600 hours. The material turned yellow and developed a sticky surface, and chemical analysis revealed that some cross-linking had occurred, generating an insoluble gel phase. By contrast, a control sample of Elvax 150 aged in the dark at 30°C experienced no changes. Specimens of cured A-9918 EVA exposed to 6 suns UV for 1400 hours at 30°C experienced only two detected changes: depletion of the residual Lupersol 101

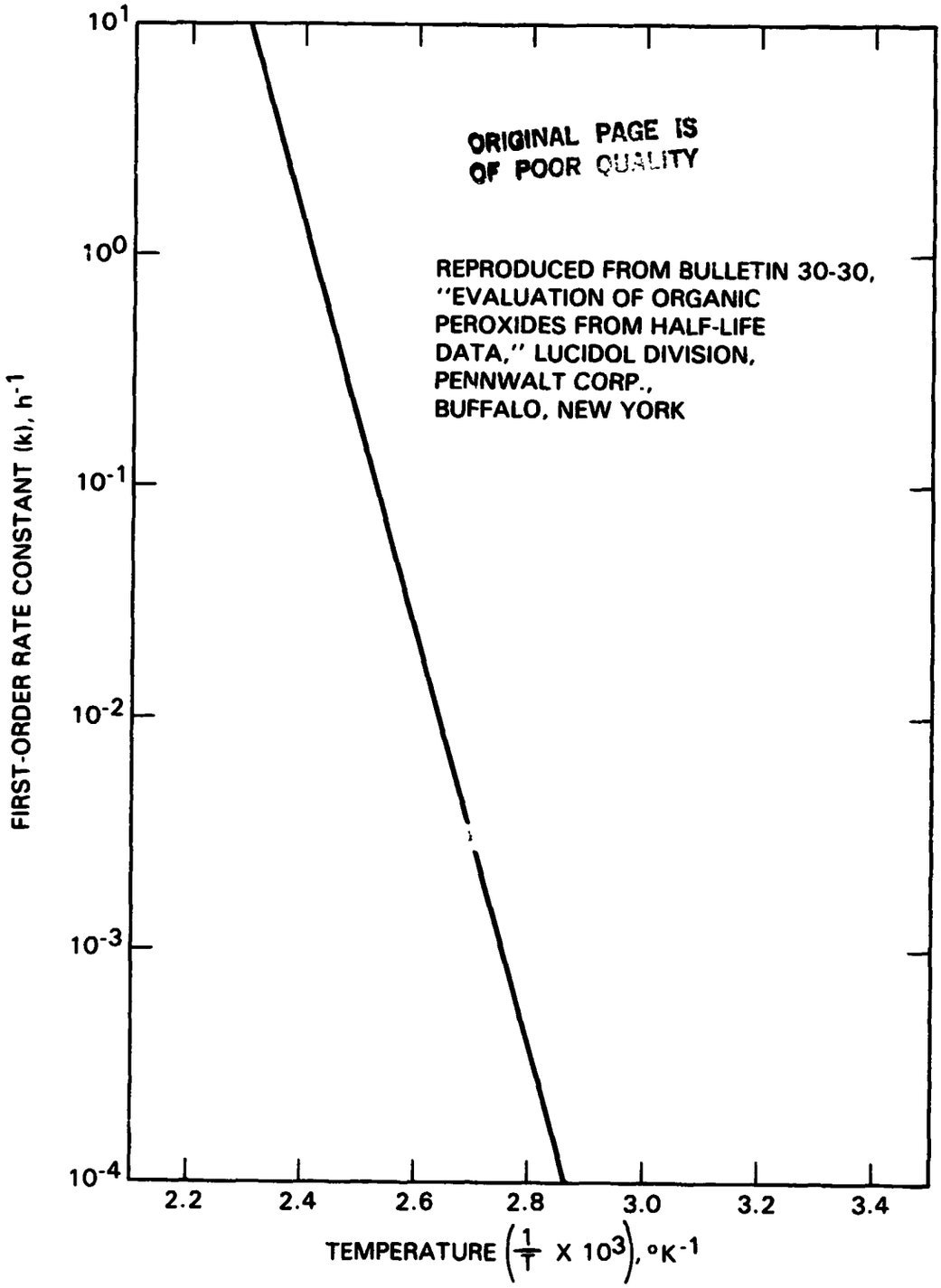

Figure 23. Thermal Decomposition of Lupersol 101 Peroxide

peroxide curing agent, and trace formation of hydroxyl groups. By contrast, a control sample of cured A-9918 aged in the dark for 1400 hours at 30°C experienced no detectable changes of any kind, including the residual peroxide

curing agent. This is readily explainable, as extrapolation of the Lupersol 101 thermal decomposition rate curve to 30°C (Figure 23) yields a halflife estimate for thermal decomposition of more than 5000 yr. The apparent stability of the Lupersol 101 against thermal decomposition in the dark at 30°C is not surprising. On the other hand, the Lupersol 101 in the A-9918 EVA exposed to 6 suns UV at 30°C rapidly decomposed, as shown in Figure 24, which is a plot of Lupersol 101 concentration versus irradiation time (Reference 10). The initial concentration of residual peroxide is about 0.13 wt %, which decays to virtually zero concentration within 50 to 60 hours. The data curve of Figure 24 is replotted semi-logarithically in Figure 25, yielding a straight line, which suggests that the UV-enhanced decomposition reaction is first-order. The estimated half-life from this figure is 15 hours for the UV-enhanced decomposition, which can be compared with the half-life estimate of more than 5000 yr for thermal decomposition at 30°C. The transient yellowing associated with the UV-enhanced peroxide decomposition peaked in about 80 to 90 hours of irradiation, and essentially decayed to zero within 200 hours. Some of the Lupersol 101 decomposition products are alcohols, which may account for the hydroxyl groups detected in the UV-exposed A-9918 EVA.

Samples of cured A-9918 EVA exposed to 6 suns of UV for 400 hours at 70°C and for 800 hours at 85°C survived in excellent condition. Specimens exposed to UV at both temperatures experienced the UV-enhanced decomposition of the Lupersol 101 peroxide. No yellowing associated with UV photooxidation or thermal oxidation was detected in specimens UV-exposed at either 70°C or 85°C. These results indicate that the Cyasorb UV-531 in the concentration used (0.3 wt %) is adequate to protect the EVA against UV-activated reactions, even at 6 suns of UV intensity. Therefore, if it is assumed that the UV protection afforded by the Cyasorb UV 531 reduced the aging of cured A-9918 EVA at 85°C to that of thermal aging only, then 800 hours of survivability at 85°C is expected on the basis of the survivability of the A-9918 EVA after a longer period of 10 mo (7200 hours) of thermal aging at Springborn.

Control samples of cured A-9918 EVA thermally aged in the dark for 400 hours at 70°C and for 800 hours at 85°C were in excellent condition, with no detection of any yellowing associated with thermal oxidation. No transient yellowing associated with the peroxide decomposition was detected, not surprisingly, as the estimated half-life (Figure 23) for thermal decomposition at 70°C is more than 23,000 hours, and is more than 1700 hours at 85°C. Samples of cured A-9918 sandwiched between the UV-filtering Pyrex glass covers and exposed to 6 suns UV for 400 hours at 70°C and for 800 hours at 85°C also survived in excellent condition. Transient yellowing associated with peroxide decomposition was not detected in these samples, providing a clue that it may be avoided in hermetically sealed superstrate designs.

Aging of cured A-9918 EVA at 105°C, however, resulted in most of the measurable and observable changes from which fundamental chemical information on A-9918 EVA aging can be currently derived. The yellowing behavior (Figure 26) of the samples thermally aged in the dark, and for those samples exposed to 6 suns of UV, both direct and those between the Pyrex glass covers, exhibited the low-intensity transient yellowing associated with the decomposition of the residual Lupersol 101 peroxide curing agent. The half-life for the thermal decomposition of Lupersol 101 at 105°C is in the order of 90 hours, and the peak yellowing intensity (minimum transmission) occurred at

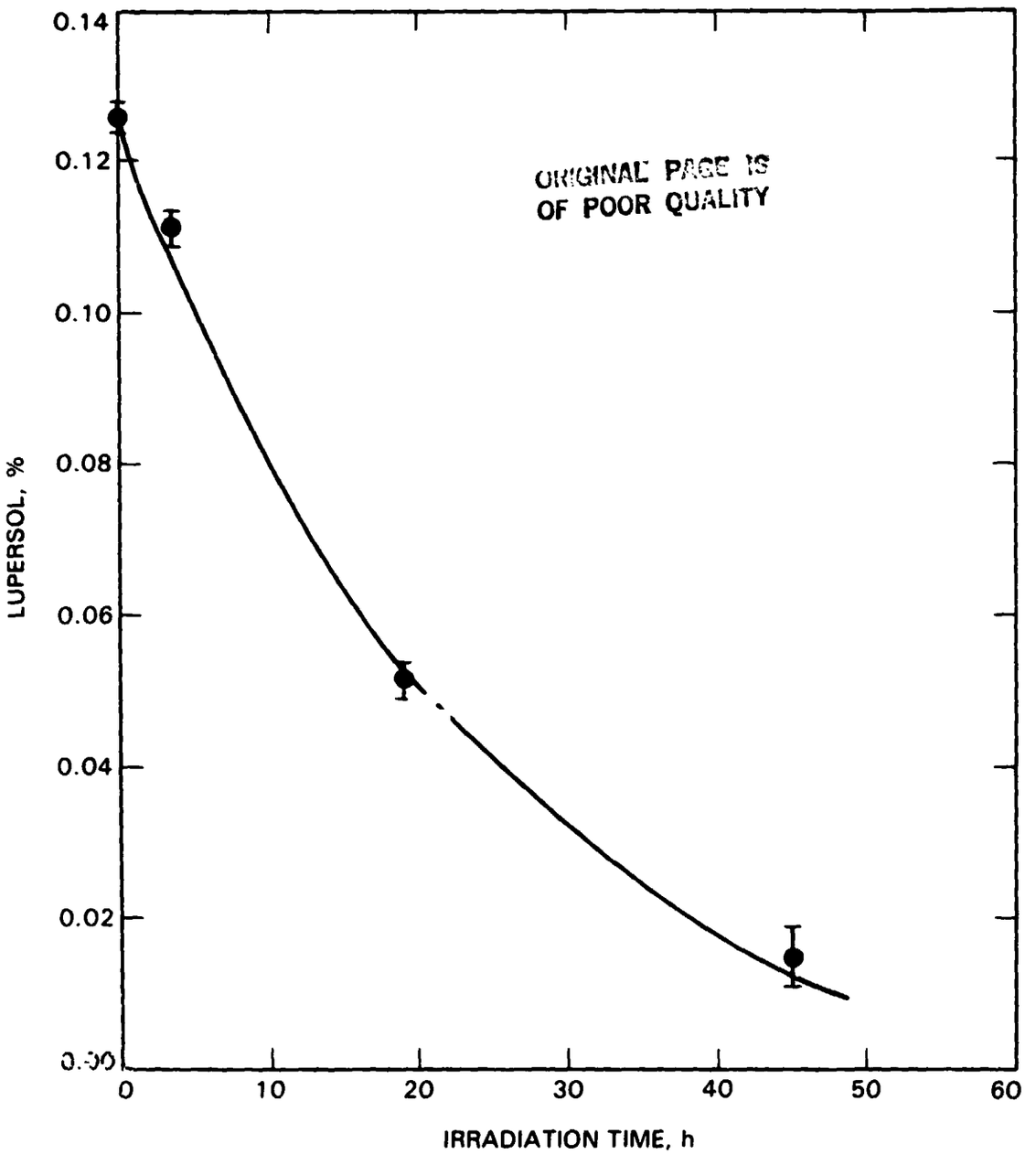

Figure 24. Concentration of Residual Lupersol 101 Peroxide Curing Agent in EVA A-9918 as a Function of Photothermal Aging at 6 suns, 30°C, in Air

about 100 hours to 120 hours. Thereafter, the transient yellowing gradually disappeared. Chemical analysis of these aged specimens identified the presence of hydroxyl groups, and barely detected minute traces of acetic acid. The hydroxyl groups may be associated with the alcohols generated from Lupersol 101 decomposition products, and with the acetic acid from the thermal

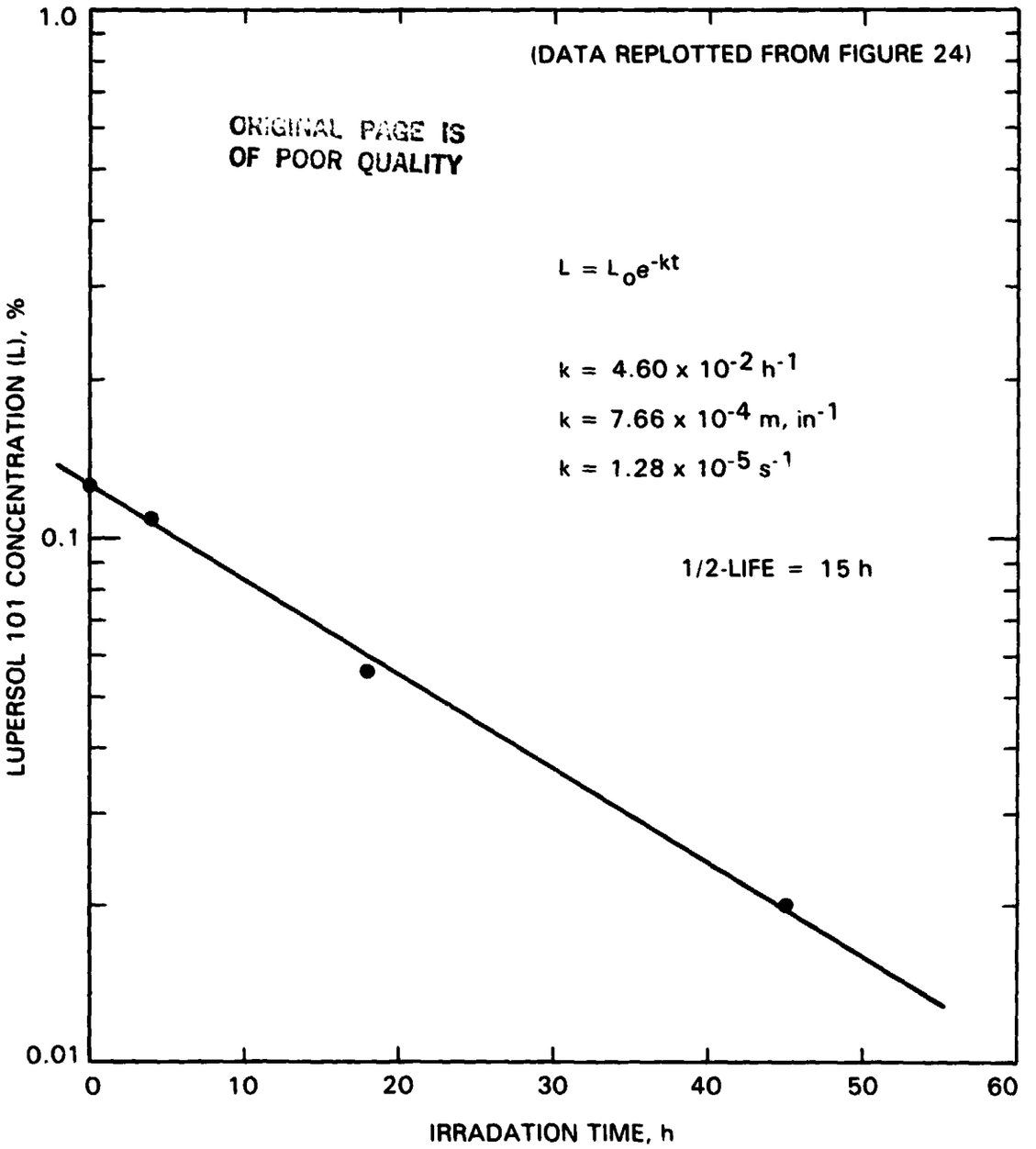

Figure 25. Depletion of Lupersol 101 From Crosslinked EVA A-9918 at 30°C, 6 suns in Air-Circulated Oven

degradation of the acetate groups in the EVA. Over the time period of this test exposure, no yellowing from either photooxidation or thermal oxidation was detected for the cured A-9918 EVA specimens sandwiched between the Pyrex glass covers.

The yellowing of the A-9918 EVA specimens thermally aged in the dark at 105°C began early in the aging test, and progressed to become increasingly intense with continued aging. Although not separately resolved, it is speculated that the early onset of yellowing is associated with the transient peroxide yellowing, and that the later, more intense yellowing is associated with thermal oxidation. No specific test to analyze chemically for the antioxidant concentration in these specimens as a function of aging time was made, and therefore its role in the oxidation process is not known. The evidence suggests that the antioxidant was very rapidly consumed, therefore providing only brief protection. It is known that the protective lifetime of an antioxidant, called the induction period, decreases with increasing temperature. The absence of visible yellowing in A-9918 EVA specimens thermally aged up to 10 mo (7200 hours) at 90°C in the Springborn test, and the development of visible yellowing within a few hundred hours at 105°C suggest the following, or combinations of the following:

(1) The protective induction period of the antioxidant decreases rapidly over the 15°C range from 90°C to 105°C.

(2) The tendency for physical loss increases rapidly over the 15°C range from 90°C to 105°C.

(3) The natural resistance of Elvax 150 to thermal oxidation may decrease sharply at some threshold temperature between 90°C and 105°C.

Detailed studies in these activity areas are being initiated, which will include longer-term thermal aging at temperatures such as 85°C and 90°C. A concern, for example, is that the 10 mo of thermal aging at 90°C may still have been within the protective induction period of the antioxidant.

The apparent absence of oxidative yellowing at 105°C of the A-9918 EVA specimens sandwiched between the Pyrex glass covers, in contrast with the rapid oxidative yellowing of the dark-thermally aged specimens, is believed to be related to adequate UV filtering by the Pyrex glass, and to the restricted access of oxygen influx and possibly antioxidant outflux at the narrow open edge of the sandwich specimens. For example, no acetic acid was detected chemically in the samples that were thermally aged in the dark at 105°C, yet there is no reason to believe that some acetic acid was not liberated. It is presumed that the liberated acetic acid was volatilized out of these specimens, but not out of the sandwich specimens because of restricted access.

The yellowing of cured A-9918 EVA directly exposed to 6 suns UV at 105°C, as shown in Figure 26, began early in the aging exposure, became quickly visible, and to about 250 hours was yellowing at a rate faster than the specimens being thermally aged in the dark. At 250 hours of exposure, a reversal in yellowing occurred, and the A-9918 EVA began to lose its yellow color and to become progressively clearer. Simultaneously, absorbance at 360 nm was decreasing (which also began early in the aging exposure) with the interpretation that Cyasorb UV-531 was being lost. The early and more rapid onset of yellowing is thought to be possibly related to the transient yellowing associated with the rapid, UV-accelerated decomposition of the residual Lupersol 101 peroxide curing agent. Thereafter, and although not completely studied, the current evidence suggests that the visible yellowing is still the

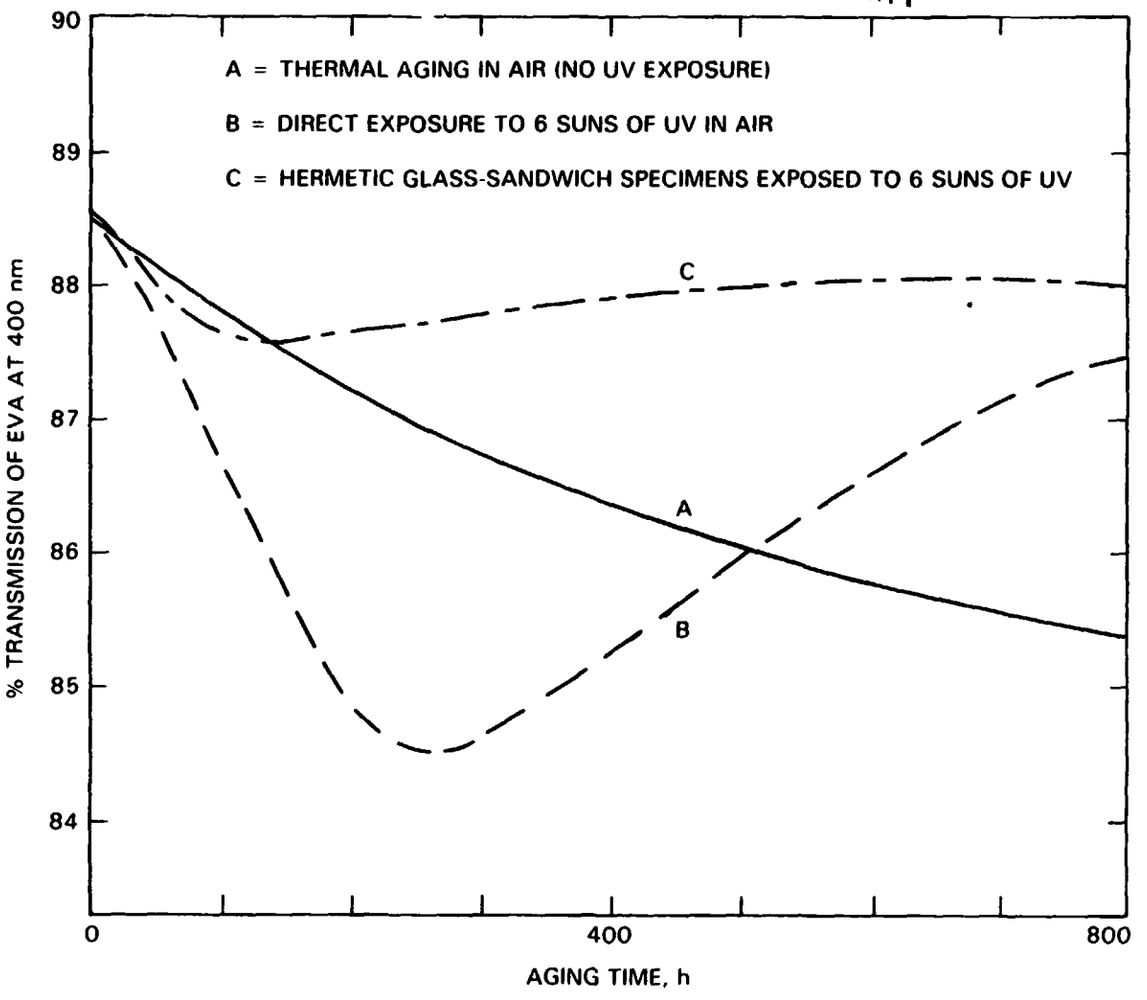

Figure 26. Change in Percentage of Transmission at 400 nm of EVA A-9918 Films as a Function of Dark Thermal Aging at 105°C, and of Photothermal Aging at 6 suns, 105°C

result of thermal oxidation, which is not appreciably accelerated by UV radiation despite gradual loss of the Cyasorb UV-531. The point is that the UV wavelengths deleterious to Elvax 150 appear to be those less than 360 nm, and since Cyasorb UV-531 absorbs up to 370 nm, gradual loss would permit gradual penetration of wavelengths which admittedly would be progressively shorter and shorter than 370 nm but still would provide UV protection until a sufficient loss of Cyasorb UV-531 had occurred to permit penetration by wavelengths $\leq$ 360 nm. Rather, the evidence suggests that UV wavelengths somewhere between 310 and 370 nm, now penetrating the oxidized EVA because of partial loss of the Cyasorb UV-531, act in turn to photooxidize the yellow thermal oxidation products, the result of the reaction being yet another degradation product that does not have a visible color -- in other words, UV bleaching.

The experimental aging data at 105°C also detected depletion of Cyasorb UV-531 from the cured A-9918 EVA specimens being thermally aged in the dark; in these specimens, however, there would be no UV bleaching. At the lower aging temperatures of 85°C, 70°C, and 30°C, the rates of depletion of Cyasorb UV-531 are apparently so much slower, if they exist, that a positive verification of loss over the aging time periods could not be made in these tests.

4. Aging Summary

Elvax 150 can be degraded by UV photooxidation, thermal oxidation, and by purely thermal decomposition of the acetate groups to acetic acid. These degradation reactions are stated in order of decreasing severity, and as protection against each in order is provided, the life and associated peak service temperature of EVA encapsulant can be extended.

Fundamental analysis of Elvax 150 suggests that the UV wavelengths deleterious to this material, and necessary for UV photooxidation, are those shorter than 360 nm. Isolation of Elvax 150 from these UV wavelengths, with UV-filtering outer covers and/or compounding additives such as Cyasorb UV-531, stops UV photooxidation, and reduces the aging characteristics of Elvax 150 to thermal effects. This basic and very simple concept was established as a fundamental module design philosophy, and no problem with this concept has been identified in the experimental aging results to date.

For example, testing of EVA samples in the RS/4 UV chambers at 55°C included the following combinations:

(1) Elvax 150 without any protection, either additives or UV-screening film overlays.

(2) Elvax 150 with a UV-screening film overlay, but having no antioxidant or UV-absorbing additives.

(3) Fully compounded and cured A-9918 EVA, having an antioxidant and UV-absorbing additive, but with no UV-screening film overlay.

The Elvax 150 sample (No. 1) without any protection yellowed visibly and degraded within 1000 h of exposure, whereas samples Nos. 2 and 3 with UV protection as indicated have to date survived 20,000 h to 30,000 h of exposure without any degrading incidences. Accepting that the UV protection for these latter two samples acted to isolate or protect them from deleterious UV wavelengths, then their aging at 55°C was reduced to that of thermal aging. And further, as no aging effects were detected in these two samples, with or without an antioxidant, these tests indicate strongly that Elvax 150 at 55°C is either naturally resistant to thermal oxidation, or undergoes negligibly slow thermal oxidation.

If it can be assumed that a module having Elvax 150 as a pottent provides the necessary UV protection, and if it can be assumed that such a module may be at or near a daily array peaking temperature of 55°C for about 5 h each day, then 20,000 h to 30,000 h of accumulated thermal aging in the RS/4 chambers corresponds to 11 to 16 years of potential outdoor service. For module applications having daytime peaking temperatures near 55°C, it appears that the life of the EVA encapsulant is related more to the life of

the UV protection schemes and less to either the thermal behavior of the EVA or thermal protection schemes (for example, antioxidants).

Between 55°C and 93°C (200°F) there is no direct experimental or literature information on the thermal aging behavior of Elvax 150. Unresolved questions relate to knowing if a threshold temperature exists for Elvax 150, above which thermal oxidation begins, to knowing the temperature-dependence of the rates of thermal oxidation of Elvax 150, and to knowing the effectiveness of antioxidants and the associated temperature-dependence of their protective induction periods. Although the 10 mo (7200 hours) of thermal stability observed at 90°C for the dark-thermal aging of cured A-9918 EVA is encouraging, it is not known whether this is natural to the Elvax 150, or that 10 mo was still within the protective induction period of the antioxidant. In addition, the concentration of Cyasorb UV-531, a critical element of the UV protection scheme, was not monitored in these thermally aged specimens.

The potential for long service life of EVA in modules at rooftop temperatures (e.g., 85°C) looks encouraging, but predictions of lifetime would be premature. As at 55°C, UV protection and permanence of the UV protection is a must. After that, it is not clearly established which of the thermally driven processes is most critical. These processes include the basic thermal oxidation properties of the Elvax 150, of antioxidants and the associated temperature dependency of their protective induction periods, and the temperature dependence of any physical loss and depletion of the protective compounding additives themselves, such as the UV and thermal stabilization additives.

The phenomenon of the UV bleaching of the yellow thermal oxidation products, observed in accelerated testing at 105°C, suggest possibilities for reducing the amount of UV filtering as currently employed in order to permit some of the UV bleaching wavelengths to penetrate throughout the EVA. In this way, allowable service temperatures of the EVA might be raised, permitting physical and mechanical deterioration by thermal oxidation to proceed at known rates related to lifetime expectations, but maintaining optical clarity by the UV bleaching effect.

A program to identify physical-loss mechanisms of the EVA compounding additives is being initiated, and the first activity of this program is intended to assess the high-temperature volatility of all of these materials. A preliminary experiment with Cyasorb UV-531 at 90°C has been carried out (Reference 15). For this preliminary experiment, 20 g of Cyasorb UV-531 in a 3-in.-dia aluminum dish was put into an air-circulated oven set at 90°C, and the weight of the material was measured periodically. The weight loss data are given in Table 17. This preliminary experiment also included an evaluation of the barrier properties of Acrylar and Tedlar plastic films in retarding or stopping the volatile loss of Cyasorb UV-531. In this experiment, standard 3-in.-dia aluminum perm-cups containing 20 g each of Cyasorb UV-531 were covered with the plastic films. The perm-cups are equipped with a perimeter gasket and clamp fixture in order to seal the edges against direct leakage. The weight loss data for the volatile loss through the Acrylar and Tedlar films are also given in Table 17.

Table 17. Volatile Loss of Cyasorb UV-53 at 90°C

Days, 90°C	Weight Loss, % Tedlar 100BG30UT	Acrylar X-22417	Control
3	0.5	0.5	0.45
7	0.7	0.65	0.75
10	0.7	0.71	0.80
14	0.75	0.77	1.00
18	0.75	0.77	1.00
22	0.75	0.81	1.11
26[a]	0.71	0.68	1.06
30	0.86	0.83	1.25
34	0.91	0.86	1.25
38	0.89	0.88	1.36

[a]The gain in weight at this point correlated with a change in ovens; the cause is not known.

In all three experiments, a more volatile but unknown component or components accounting for about 0.5 wt % of the sample was rapidly boiled off within the first three days, and thereafter the evaporative weight-loss behavior became essentially linear with time. The steady-state rate of loss of Cyasorb UV-531 from the uncovered control cup averaged about 0.14 wt % per week, and about 0.048 wt % per week from the covered cups. These preliminary data demonstrated that Cyasorb UV-531 is volatile at 90°C, but at a very low rate, and that the UV filtering plastic films would only slow but would not stop migration and volatile loss of Cyasorb UV-531.

H. ADVANCED EVA STUDIES

The available evaluation-ready EVA (A-9918) has been received favorably by the industry. However, its status is still considered to be experimental. To advance EVA toward application readiness, several developmental tasks to improve on quality and durability remain to be completed:

(1) Faster processing, primarily in the cure schedule, which involves a reduction in cure time and temperature; the minimum cure temperature will be dictated by the requirement that the curing system must not become active during film extrusion.

(2) Optimization of the UV-stabilization additives and achievement of resistance against physical loss; the present additives were selected based on literature citation and industrial experience with polymers similar to EVA.

(3) Identification of the peak-service temperature allowed for EVA in a module application, to ensure 20-yr life.

(4) Industrial evaluation of the desirability of having a self-priming EVA, recognizing the possibility of an additional cost component (cost-benefit-performance trade-off).

Briefly described herein are some of the early considerations and/or experimental trends relative to the first two of those tasks, (1) and (2). Not discussed herein, but planned, are extended experimental studies of the currently used antioxidant, in order to identify the limits of its protective capabilities, and to identify and evaluate, if necessary, potentially higher performance antioxidant materials.

1. Curing Agent Studies

These studies are intended to identify alternative peroxide curing agents that would reduce cure times and temperatures, as compared with Lupersol 101, in order to realize a faster lamination cycle at lower temperatures for higher-volume fabrication operations. In addition, there appear to be room-temperature shelf-life limitations associated with the use of Lupersol 101. It has been observed that A-9918 EVA slowly loses its ability to cure if it is stored as unrolled cut sheet. Further, this tendency to lose curability has been observed for the outer layer of rolled EVA. The time in which this behavior manifests itself can be in the order of a few days to several weeks. It is speculated that this behavior may be a result of a gradual volatile loss of the Lupersol 101, or from rapid decomposition of the Lupersol 101 resulting from exposure to short-wavelength UV light (<360 nm), which may be generated by room lighting. Occasionally a faint yellow color is observed in uncured A-9918 EVA film that is exposed to room lighting; as observed in the EVA aging studies, this may be associated with the decomposition of the Lupersol 101.

Three other peroxide curing agents, all available from the Lucidol Division of the Pennwalt Corp., Buffalo, NY, are being investigated. Their commercial designations are:

(1) Lupersol 99.

(2) Lupersol 331-80B.

(3) Lupersol TBEC.

These agents were substituted for the Lupersol 101 in the A-9918 EVA (see Table 3) and were used at the same concentration of 1.5 phr as used for the Lupersol 101. The modified A-9918 EVA containing these peroxide curing agents were cured at various combinations of time and temperature, and the efficiencies of cure were monitored by measurement of the resultant gel content of the cured EVA.

The cure data for these three peroxide curing agents, along with Lupersol 101 cure data for comparison, are given in Table 18. Compared with Lupersol 101, all three of the other peroxides are more efficient, resulting in faster cures at lower temperatures, which achieve or exceed the minimum required gel content of 65 to 70 wt % in the cured EVA. These results indicate that, when compared to cure with Lupersol 101, one of the new peroxides may be capable of resulting in equivalent cure in 1/3 to 1/10 the time, depending on the temperature selected. A high degree of cure at a lower temperature is desirable because of energy savings and reduced time required for heat transfer during lamination. For example, the recommended cure condition for A-9918 EVA with Lupersol 101 is 10 to 15 min at 150°C, in order to achieve the minimum required gel content. This same level of gel content can be achieved in 10 to 15 min at 120°C with Lupersol 331-80B, or with any of the three alternative peroxides cited above, in 5 min or less at 150°C.

A guideline for selecting peroxide curing agents as alternatives to Lupersol 101 is to recognize that the lowest temperature allowable for EVA cure is dictated by the requirement that no cure of the compounded EVA occur during film extrusion. As the temperature of the EVA within the barrel of the film extruder can be at a temperature of 115°C for a few minutes, the use of a curing agent that would result in measurable cure at this temperature is to be avoided. Allowing for a safety margin of about 5°C above the peak extrusion temperature establishes an allowable lower-bound cure temperature of about 120°C. Thus, of the three peroxides evaluated to date, and solely on the basis of cure data, Lupersol 331-80B would appear to be the choice as an alternative to Lupersol 101.

However, if it is assumed that one of the shelf-life limitations of A-9918 EVA formulated with Lupersol 101 is related to volatile loss of this peroxide, then an alternative peroxide should also be less volatile compared with Lupersol 101. All four of these Lupersol peroxides are liquids, but their boiling points cannot be measured because chemical decomposition occurs before any evidence of boiling is observed. Further, vapor pressure at room temperature has not been measured, nor found in published literature. However, the flash points of each of these four peroxide liquids are given in Pennwalt technical sales literature for these products; these flash points are listed in Table 19. If it can be assumed that comparison of flash points provides a relative measure of volatility, then Lupersol 331-80B is unfortunately the most volatile of the four, and Lupersol TBEC is the least volatile. Comparing the flash points of Lupersol 101 and Lupersol 331-80B suggest comparable volatility, and thus, although substitution of Lupersol 331-80B for Lupersol 101 may result in faster curing at lower temperatures, improvements in shelf life may not be realized; it may even be worse. Therefore, based on volatility behavior suggested by flash-point data, Lupersol TBEC becomes a preferred alternative to Lupersol 101.

Continuing work with these and other curing agents yet to be identified will involve vapor-pressure measurements, shelf-life characteristics, and effects, if any, of the alternate curing agents on module fabricability, other compounding additives, efficiency and performance of adhesives and primers developed for EVA, and weather aging of EVA encapsulated modules.

Table 18. Cure of A-9918 EVA at Various Times and Temperatures with Four Different Peroxide Curing Agents as Monitored by Gel Content in wt %

Lupersol 101

Cure Time, min	Degree of Cure, % Gel				
	130°C	140°C	150°C	160°C	170°C
1			0	2.1	28.8
2		1.0	4.1	29.5	74.2
5		11.8	21.1	73.0	81.2
10	1.0	23.5	63.2	82.6	92.7
15	2.3	59.3	88.3		
30	3.4	68.2			
60	32.1	80.6			

Lupersol 99

Cure Time, min	Degree of Cure, % Gel					
	110°C	120°C	130°C	140°C	150°C	160°C
2					low	75.2
5				low	70.7	79.0
10	0	low	low	72.2	77.7	79.9
15	0	8.1	69.5	74.9	78.4	
30	low	76.0	82.1	77.7	79.9	

Table 18. Cure of A-9918 EVA at Various Times and Temperatures with Four Different Peroxide Curing Agents as Monitored by Gel Content in wt % (Cont'd)

Lupersol 331-80B

Cure Time, min	Degree of Cure, % Gel					
	110°C	120°C	130°C	140°C	150°C	160°C
2					79.5	84.5
5				88.8	86.9	88.7
10	0	68.2	84.2	89.3	88.0	87.6
15	0	80.4	87.4	92.4	88.9	
30	0	78.5	92.0	89.9		

Lupersol TBEC

Cure Time, min	Degree of Cure, % Gel			
	120°C	130°C	140°C	150°C
2	0	0	73.4	81.5
5	0	60.3	83.7	88.6
10	0	75.0	88.2	91.6
15	0	85.0	90.2	93.5
20	60	78.3	92.7	93.0
30	-	82.7	92.2	92.6

2. UV-Absorbing Additives

The EVA aging studies described in this paper strongly indicate that UV protection of the EVA is essentially assured as long as the Cyasorb UV-531 UV-absorbing additive remains physically within the EVA. However, the aging studies carried out at 105°C indicate a tendency toward gradual physical loss of this additive, presumably by volatility.

Table 19. Flash Points of the Four Lupersol Peroxide Curing Agents

Peroxide	Flash Point (Volatility)
Lupersol 101	43°C
Lupersol 331-80B	40°C
Lupersol 99	77°C
Lupersol TBEC	101°C

A major premise for the durability of low-cost, UV-sensitive pottants is that protection will be ensured by UV filtering through the glass superstrate, or through UV-screening plastic-film front covers, and that any harmful UV that does pass through the filters will be absorbed harmlessly within the pottant itself by uniformly dispersed UV screening agents. Loss of UV protection for the pottant by either chemical consumption of the screening agents or by physical loss from bleeding, migration, rainwater leaching, etc., could limit module longevity.

Fortunately, commercial UV screening agents in widespread use, and those used in the pottants and front-cover plastic films, are not susceptible to chemical consumption. They are not chemically destroyed when absorbing UV radiation; rather, they convert UV photon energy into heat. Thus these agents perform their UV-screening function as long as they are retained in the film and/or the pottant.

UV screening agents can be divided into two classes: those that are only physically dispersed throughout the bulk volume of a carrier medium, and those that are dispersed throughout the bulk volume of the carrier medium and also are chemically bound to the carrier. Those that are only physically dispersed can be further classified on the basis of their molecular weight, or on the basis of whether they are small molecules or polymer molecules.

Small-molecule UV-screening agents such as Cyasorb UV-531 are the most susceptible to physical loss by migration, bleeding, evaporation, leaching, etc. Efforts to diminish these physical-loss tendencies by making the molecules bigger, but not polymeric, increases the problem of uniform dispersal compatibility because the UV screening agents tend to agglomerate into tiny discrete globules. If this occurs in a pottant, no protection may be afforded. Thus there is an inverse relationship between uniform dispersal and molecule size.

Although the physical-loss tendencies for small-molecule UV screening agents are recognized, it is important to also recognize that a pottant will be sandwiched between front and back-covering materials, thereby introducing some partial or total barrier resistance to physical loss of the UV screening agents. No physical loss is expected for a glass-superstrate module with a

metal-foil back cover. However, a loss possibility exists for a design with other than a metal-foil back cover and for a substrate design with a plastic-film front cover.

At this state in developing encapsulation technology for specific additives, it cannot be stated with any certainty that deleterious losses can be predicted over the 20-yr desired lifetime of terrestrial modules.

Thus, a program to develop and evaluate permanent UV screening by chemical attachment has become a major activity. Table 20 summarizes three monomeric chemically attachable UV screening agents of present interest. Permasorb MA is available in limited quantities from National Starch and Chemicals Corp.; vinyl tinuvin is just barely out of the laboratory, with small quantities being produced at Springborn, and the 2-hydroxy-3-allyl-4,4'-dimethoxybenzophenone is still at the laboratory development level. Preliminary work suggests that vinyl tinuvin will chemically attach to EVA without difficulty.

An additional approach is to produce polymeric UV absorbers, copolymerizing the monomeric UV screening agent (see Table 20) with a polymeric material that is compatible with the intended carrier medium. Efforts are still at the laboratory level. Physically dispersed polymeric UV screening agents should be significantly more resistant to physical-loss mechanisms than are small-molecule UV screening agents.

Table 20. Chemically Attachable Ultraviolet Screening Agents

Agent	Status	Source
Permasorb MA	Limited availability	National Starch and Chemical Corp.
Vinyl Tinuvin	Laboratory-scale production	Asahi Chemicals; University of Massachusetts; Springborn
2-hydroxy-3-allyl-4,4'-dimethoxybenzophenone	Experimental	JPL

REFERENCES

1. Willis, P., et al., Investigations of Test Methods, Material Properties, and Processes for Solar-cell Encapsulants, Annual Report, ERDA/JPL-954527, Springborn Laboratories, Inc., Enfield, Connecticut, July 1977.

2. Cuddihy, E.F., Encapsulation Material Trends Relative to 1986 Cost Goals, JPL Document No. 5101-61, Jet Propulsion Laboratory, Pasadena, California, April 13, 1978.

3. Willis, P., Baum, B., and White, R., Investigations of Test Methods, Material Properties, and Processes for Solar-Cell Encapsulants, Annual Report, ERDA/JPL-954527, Springborn Laboratories, Inc., Enfield, Connecticut, July 1978.

4. Cuddihy, E.F., Baum, B., and Willis, P., Low-Cost Encapsulation Materials for Terrestrial Solar Cell Modules, JPL Document No. 5101-78, Jet Propulsion Laboratory, Pasadena, California, September 1978, and Solar Energy, Vol. 22, p. 389, 1979.

5. Cuddihy, E.F., Encapsulation Materials Status to December 1979, JPL Document No. 5101-144, Jet Propulsion Laboratory, Pasadena, California, January 15, 1980.

6. Willis, P., and Baum, B., Investigations of Test Methods, Material Properties, and Processes for Solar-Cell Encapsulants, Annual Report, ERDA/JPL-954527, Springborn Laboratories, Inc., Enfield, Connecticut, July 1979.

7. Willis, P., et al., Investigations of Test Methods, Material Properties, and Processes for Solar-Cell Encapsulants, Annual Report, ERDA/JPL-954527, Springborn Laboratories, Inc., Enfield, Connecticut, July 1980.

8. Cuddihy, E., et al, Photovoltaic Module Encapsulation Design and Materials Selection: Volume I, JPL Publication 81-102, JPL Document No. 5101-177, DOE/JPL-1012-56, Jet Propulsion Laboratory, Pasadena, California, June 1, 1982.

9. Spectrolab, Inc., Phase I Technical Report for FSA Contract 955567, November 1981.

10. Liang, R., et al, Photothermal Characterization of Encapsulant Materials for Photovoltaic Modules, JPL Publication 82-42, JPL Document No. 5101-210, DOE/JPL-1012-72, Jet Propulsion Laboratory, Pasadena, California, June 1, 1982.

11. Stultz, J.W., and Wen, L. C., Thermal Performance Testing and Analysis of Photovoltaic Modules in Natural Sunlight, JPL Document No. 5101-31, Jet Propulsion Laboratory, Pasadena, California, July 29, 1977.

12. Stultz, J.W., Thermal and Other Tests of Photovoltaic Modules Performed in Natural Sunlight, JPL Document No. 5101-76, DOE/JPL-1012-78/9, Jet Propulsion Laboratory, Pasadena, California, July 31, 1978.

13. Griffith, J.A., Rathod, M.S., and Paslaski, J., "Some Tests of Flat Plate Photovoltaic Module Cell Temperatures in Simulated Field Conditions," presented at 15th IEEE Photovoltaic Specialists Conference, Kissimmee, Florida, May 12-15, 1981.

14. Rogers, C., "Permeability and Chemical Resistance," Chapter 9 in Engineering Design for Plastics, E. Baer, editor, Reinhold Publishing Co., New York, 1964.

15. Willis, P., et al, Investigation of Test Methods, Material Properties, and Processes for Solar-Cell Encapsulants, Annual Report, ERDA/JPL-954527, Springborn Laboratories, Inc., Enfield, Connecticut, July, 1981.

16. Duncan, R.E., and Bergerhouse, J.E., "EVA and VAE Copolymers for Hot Melt PSA's," Adhesives Age, pp. 37-41, March 1980.

17. The Vanderbilt Rubber Handbook, edited by George G. Winspear, R.T. Vanderbilt Co., Inc., New York, 1968.

18. Allen, G., Gee, G., and Wilson, J., Polymer, Vol. 1, p. 456, 1960.

19. Fox, T.G., Bulletin of the American Physical Society, Vol. 1, No. 3, p. 123, 1956.

20. Polyethylene, Edited by R.A.V. Raff and J.B. Allison, High Polymer Series, Volume XI, Interscience Publishers, Inc., New York, (1952).

21. Myers, C.S., J. Polymer Science, Vol. 13, pp. 549-564, 1951.

22. Pleuddemann, E.P., Chemical Bonding Technology for Terrestrial Solar Cell Modules, JPL Document No. 5101-132, Jet Propulsion Laboratory, Pasadena, California, September 1, 1979.

23. Chen, C.P., Fracture Strength of Silicon Solar Cells, JPL Publication 79-102, JPL Publication 79-102, JPL Document No. 5101-137, DOE/JPL-1012-32, Jet Propulsion Laboratory, Pasadena, California, October 15, 1979.

24. Cuddihy, E.F., Development of Reduced-Variable Master Curves for Estimating Tensile Stresses of Encapsulated Solar Cells Caused by Module Deflection or Thermal Expansion, JPL Document No. 5101-182, Jet Propulsion Laboratory, Pasadena, California, October 1, 1981.

25. Hoffman, A.R., and Maag, C.R., "Airborne Particulate Soiling of Terrestrial Photovoltaic Modules and Cover Materials," Proceedings of the Institute of Environmental Sciences, Philadelphia, Pennsylvania, May 11-14, 1980, Institute of Environmental Sciences, Mt. Prospect, Illinois, 1980.

26. Hoffman, A.R., and Maag, C.R., Photovoltaic Module Soiling Studies, May 1978 to October 1980, JPL Publication 80-87, JPL Document 5101-131, DOE/JPL-1012-49, Jet Propulsion Laboratory, Pasadena, California, November 1, 1980.

27. Cuddihy, E.F., "Theoretical Considerations of Soil Retention," Solar Energy Materials, Vol. 3, pp. 21-33, 1980.

28. Photovoltaic Module Design, Qualification and Testing Specification, JPL Document No. 5101-65, DOE/JPL-1012-78/7A, Jet Propulsion Laboratory, Pasadena, California, March 24, 1978.

29. Block V Solar Cell Module Design and Test Specification for Residential Applications--1981, JPL Internal Document No. 5101-161, Jet Propulsion Laboratory, Pasadena, California, February 20, 1981.

30. Estey, R.S., Measurement of Solar and Simulator Ultraviolet Spectral Irradiance, JPL Internal Document No. 5101-58, Jet Propulsion Laboratory, Pasadena, California, March 15, 1978.

31. Terrestrial Service Environments for Selected Geographic Locations, ERDA/JPL-954328-76/5, Battelle Columbus Laboratories, Columbus, Ohio, June 24, 1976.